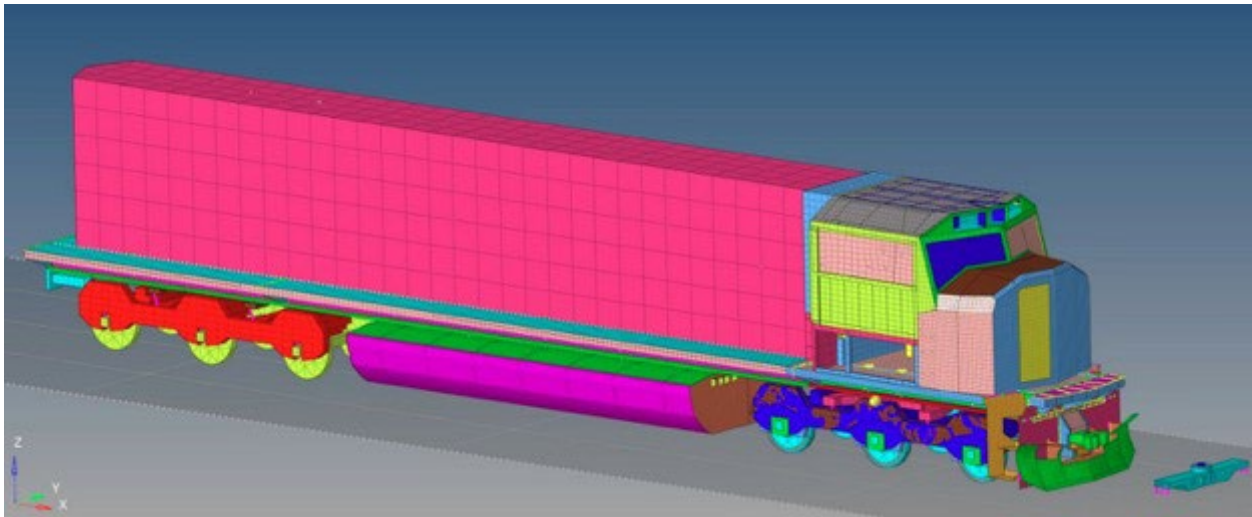




Evaluation of Modern Locomotive Crashworthiness Performance



NOTICE

This document is disseminated under the sponsorship of the Department of Transportation in the interest of information exchange. The United States Government assumes no liability for its contents or use thereof. Any opinions, findings and conclusions, or recommendations expressed in this material do not necessarily reflect the views or policies of the United States Government, nor does mention of trade names, commercial products, or organizations imply endorsement by the United States Government. The United States Government assumes no liability for the content or use of the material contained in this document.

NOTICE

The United States Government does not endorse products or manufacturers. Trade or manufacturers' names appear herein solely because they are considered essential to the objective of this report.

REPORT DOCUMENTATION PAGE

Form Approved
OMB No. 0704-0188

The public reporting burden for this collection of information is estimated to average 1 hour per response, including the time for reviewing instructions, searching existing data sources, gathering and maintaining the data needed, and completing and reviewing the collection of information. Send comments regarding this burden estimate or any other aspect of this collection of information, including suggestions for reducing the burden, to Department of Defense, Washington Headquarters Services, Directorate for Information Operations and Reports (0704-0188), 1215 Jefferson Davis Highway, Suite 1204, Arlington, VA 22202-4302. Respondents should be aware that notwithstanding any other provision of law, no person shall be subject to any penalty for failing to comply with a collection of information if it does not display a currently valid OMB control number.
PLEASE DO NOT RETURN YOUR FORM TO THE ABOVE ADDRESS.

1. REPORT DATE (DD-MM-YYYY) 05-09-2024		2. REPORT TYPE Final Report		3. DATES COVERED (From - To) 09/2021-06/2023	
4. TITLE AND SUBTITLE Evaluation of Modern Locomotive Crashworthiness Performance				5a. CONTRACT NUMBER 693JJ621C000016	
				5b. GRANT NUMBER	
				5c. PROGRAM ELEMENT NUMBER	
6. AUTHOR(S) Dr. Kelly Ozdemir: ORCID # 0000-0002-3238-4163 Dr. Fadi Tahan: ORCID # 0009-0006-3741-8074 Dr. Dhafer Marzougui: ORCID # 0000-0003-1514-4552 Dr. Abdullatif (Bud) Zaouk: ORCID # 0000-0003-3344-5412 Dr. Tarek Omar: ORCID # 0000-0002-3969-1406				5d. PROJECT NUMBER	
				5e. TASK NUMBER	
				5f. WORK UNIT NUMBER	
				8. PERFORMING ORGANIZATION REPORT NUMBER DUNS 080315515	
7. PERFORMING ORGANIZATION NAME(S) AND ADDRESS(ES) KEA Technologies, Inc. One Monarch Dr, Suite 100 Littleton, MA 01460				10. SPONSOR/MONITOR'S ACRONYM(S)	
9. SPONSORING/MONITORING AGENCY NAME(S) AND ADDRESS(ES) U.S. Department of Transportation Federal Railroad Administration Office of Railroad Policy and Development Office of Research, Development and Technology Washington, DC 20590				11. SPONSOR/MONITOR'S REPORT NUMBER(S) DOT/FRA/ORD-24-35	
12. DISTRIBUTION/AVAILABILITY STATEMENT This document is available to the public through the FRA website .					
13. SUPPLEMENTARY NOTES COR: Dr. Tarek Omar					
14. ABSTRACT The goal of this project is to assess crew safety of existing locomotive crashworthiness requirements using existing modern freight locomotive crash data analyses and simulation techniques. This project will evaluate the impact of the crashworthiness standards defined in Subpart D of 49 CFR Part 229, and in the AAR S-580 Locomotive Crashworthiness Requirements, on the safety performance of the modern locomotive through a combination of statistical analysis, finite element modeling and simulation, as well as validation tests.					
15. SUBJECT TERMS FRA, AAR, NTSB, 49 CFR Part 229, S-580, crashworthiness, modern locomotive, collision, finite element model, finite element analysis					
16. SECURITY CLASSIFICATION OF:			17. LIMITATION OF ABSTRACT	18. NUMBER OF PAGES 92	19a. NAME OF RESPONSIBLE PERSON Kelly Ozdemir
a. REPORT	b. ABSTRACT	c. THIS PAGE			19b. TELEPHONE NUMBER (Include area code) 508-658-9425

METRIC/ENGLISH CONVERSION FACTORS

ENGLISH TO METRIC

LENGTH (APPROXIMATE)

1 inch (in) = 2.5 centimeters (cm)
 1 foot (ft) = 30 centimeters (cm)
 1 yard (yd) = 0.9 meter (m)
 1 mile (mi) = 1.6 kilometers (km)

AREA (APPROXIMATE)

1 square inch (sq in, in²) = 6.5 square centimeters (cm²)
 1 square foot (sq ft, ft²) = 0.09 square meter (m²)
 1 square yard (sq yd, yd²) = 0.8 square meter (m²)
 1 square mile (sq mi, mi²) = 2.6 square kilometers (km²)
 1 acre = 0.4 hectare (he) = 4,000 square meters (m²)

MASS - WEIGHT (APPROXIMATE)

1 ounce (oz) = 28 grams (gm)
 1 pound (lb) = 0.45 kilogram (kg)
 1 short ton = 2,000 pounds (lb) = 0.9 tonne (t)

VOLUME (APPROXIMATE)

1 teaspoon (tsp) = 5 milliliters (ml)
 1 tablespoon (tbsp) = 15 milliliters (ml)
 1 fluid ounce (fl oz) = 30 milliliters (ml)
 1 cup (c) = 0.24 liter (l)
 1 pint (pt) = 0.47 liter (l)
 1 quart (qt) = 0.96 liter (l)
 1 gallon (gal) = 3.8 liters (l)
 1 cubic foot (cu ft, ft³) = 0.03 cubic meter (m³)
 1 cubic yard (cu yd, yd³) = 0.76 cubic meter (m³)

TEMPERATURE (EXACT)

$$[(x-32)(5/9)] \text{ } ^\circ\text{F} = y \text{ } ^\circ\text{C}$$

METRIC TO ENGLISH

LENGTH (APPROXIMATE)

1 millimeter (mm) = 0.04 inch (in)
 1 centimeter (cm) = 0.4 inch (in)
 1 meter (m) = 3.3 feet (ft)
 1 meter (m) = 1.1 yards (yd)
 1 kilometer (km) = 0.6 mile (mi)

AREA (APPROXIMATE)

1 square centimeter (cm²) = 0.16 square inch (sq in, in²)
 1 square meter (m²) = 1.2 square yards (sq yd, yd²)
 1 square kilometer (km²) = 0.4 square mile (sq mi, mi²)
 10,000 square meters (m²) = 1 hectare (ha) = 2.5 acres

MASS - WEIGHT (APPROXIMATE)

1 gram (gm) = 0.036 ounce (oz)
 1 kilogram (kg) = 2.2 pounds (lb)
 1 tonne (t) = 1,000 kilograms (kg)
 = 1.1 short tons

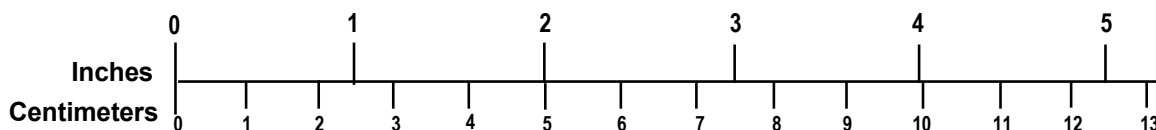
VOLUME (APPROXIMATE)

1 milliliter (ml) = 0.03 fluid ounce (fl oz)
 1 liter (l) = 2.1 pints (pt)
 1 liter (l) = 1.06 quarts (qt)
 1 liter (l) = 0.26 gallon (gal)
 1 cubic meter (m³) = 36 cubic feet (cu ft, ft³)
 1 cubic meter (m³) = 1.3 cubic yards (cu yd, yd³)

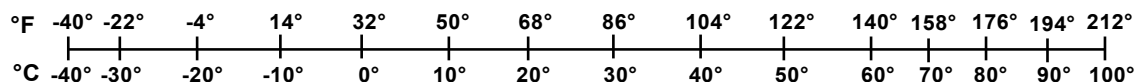
TEMPERATURE (EXACT)

$$[(9/5) y + 32] \text{ } ^\circ\text{C} = x \text{ } ^\circ\text{F}$$

QUICK INCH - CENTIMETER LENGTH CONVERSION



QUICK FAHRENHEIT - CELSIUS TEMPERATURE CONVERSION



For more exact and or other conversion factors, see NIST Miscellaneous Publication 286, Units of Weights and Measures. Price \$2.50 SD Catalog No. C13 10286

Updated 6/17/98

Contents

Executive Summary	10
1. Introduction	12
1.1 Background	12
1.2 Objective	12
1.3 Overall Approach	13
1.4 Organization of the Report	15
2. Task 1	16
2.1 Task 1 Research Methodology	16
2.2 Accident and Collision Data	18
2.3 Task 1 Conclusions	24
3. Task 2	25
3.1 Research Methodology	25
3.2 Task 2 Conclusions	28
4. Task 3 and Task 4	29
4.1 Methodology	29
4.2 FE Model Validation	40
4.3 Task 3 and Task 4 Conclusions	45
5. Task 5	47
5.1 NTSB Cases Summary	47
5.2 Updated and New FE Models	57
5.3 NTSB Crash Case RAR 13-02 Simulation	61
5.4 Task 5 Conclusions	73
6. Task 6	74
6.1 Research Methodology	74
6.2 Evaluation of S-580 Regulation Impact for Previous years	86
7. Conclusions	90
References	91
Abbreviations and Acronyms	92

Tables

Table 1. Accidents Identified from Databases Surveys	18
Table 2. Descriptions of Collisions.....	19
Table 3. Accident Severity Parameters	22
Table 4. Striking Train’s Lead Locomotive.....	23
Table 5. Struck Train’s Lead Locomotive	23
Table 6. Collision Severity Parameters and Scores	25
Table 7. Short Listed, Top Five Severe Collision Cases Based on Normalized Score.....	25
Table 8. Ranking Metric Evaluation Process Involving The 22 Accident Cases Identified in Task 1.....	26
Table 9. Available TTC Crash Tests.....	29
Table 10. Available FE Models	32
Table 11. Units and Essential Conversion between SI and Original FE Model Units	36
Table 12. Original Open-Top Hopper Car Model Characteristic	37
Table 13. Updated Open-Top Hopper Car Model Characteristics	39
Table 14. Train Crash RAR-13-02 Summary	47
Table 15. Train Crash RAR-21-01 Summary	49
Table 16. Train Crash RAR-19-02 Summary	51
Table 17. Train Crash RAR-16-03 Summary	54
Table 18. Train Crash RAR-15-02 Summary	55
Table 19. Units and Conversion Equations between SI and Original FE Model Units.....	57
Table 20. Original and Updated FE Models Details of the SD70MAC Locomotives Comparisons	58
Table 21. FE Model Details of the Ship Consist Car.....	60
Table 22. FE Model Details of the Auto-Rack Car	61
Table 23. FE Model Details of Both Trains.....	63

Figures

Figure 1. Class I Freight Locomotive Ratio of Modern to Non-Modern Locomotives.....	16
Figure 2. Accident/Incident Rates per Class I Freight Million Miles (U.S. Federal Railroad Administration, 2021).....	17
Figure 3: Number of Post-Accident In-cab Casualties of U.S. Class I Freight Railroads in Revenue Service (U.S. Federal Railroad Administration, 2021).....	17
Figure 4. Closed Hopper Car	34
Figure 5. Mass-Coastal Locomotive	35
Figure 6. The Point of Contact between the Train Car and the Truck.....	35
Figure 7. Truck to Train Connections.....	35
Figure 8. Railcar Wheel Replacement Shows the Stout Pin.....	36
Figure 9. Original Open-Top Hopper Car FE Model	37
Figure 10. Updated and Modified Open-Top Hopper Car FE Model.....	37
Figure 11. Pre-Crash Image of TTC Test 1 Hopper Car Figure	38
Figure 12. Pre-Crash Image of TTC Test 1 Hopper Car.....	38
Figure 13. Locomotive Nodal Rigid Body Constraint (Cab and Hood Not Shown).....	40
Figure 14. Original Model Setup (From TTC Test 1 Report).....	41
Figure 15. Three Consist Car Models Used Behind the Locomotive	41
Figure 16. Modified Open-Top Hopper Car FE Model.....	42
Figure 17. Close-Up of the Updated Model Setup	42
Figure 18. Overview of the Updated Model Setup	42
Figure 19. Sequential Images between Simulation and TTC Crash Test at 0 ms.....	43
Figure 20. Sequential Images between Simulation and TTC Crash Test at 200 ms.....	43
Figure 21. Sequential Images between Simulation and TTC Crash Test at 400 ms.....	43
Figure 22. Sequential Images between Simulation and TTC Crash Test at 600 ms.....	43
Figure 23. Sequential Images between Simulation and TTC Crash Test at 800 ms.....	43
Figure 24. Sequential Images between Simulation and TTC Crash Test at 1,000 ms.....	43
Figure 25. Sequential Images between Simulation and TTC Crash Test at 1,200 ms.....	44
Figure 26. Sequential Images between Simulation and TTC Crash Test at 1,400 ms.....	44
Figure 27. Sequential Images between Simulation and TTC Crash Test at 1,600 ms.....	44
Figure 28. Sequential Images between Simulation and TTC Crash Test at 1,800 ms.....	44
Figure 29. Sequential Images between Simulation and TTC Crash Test at 1,900 ms.....	44

Figure 30. Sequential Images between Simulation and TTC Crash Test at 2,000 ms.....	44
Figure 31. Post-Impact Crush Comparisons, Overview	45
Figure 32. Post-Impact Crush Comparisons, Close-Up.....	45
Figure 33. NTSB RAR-13-02 Head-On Collision Near Goodwell, OK, Overview.....	48
Figure 34. NTSB RAR-13-02, Close-Up.....	48
Figure 35. NTSB RAR-13-02, Wreckage Close-Up	49
Figure 36. NTSB RAR-21-01 BNSF Railroad Collision Near Kingman, AZ, Overview.....	50
Figure 37. NTSB RAR-21-01 BNSF Railroad Collision Near Kingman, AZ, Wreckage Close-Up	50
Figure 38. NTSB RAR-21-01 BNSF Railroad Collision Near Kingman, AZ, RUM from CWR Work Train (Source: BNSF).....	51
Figure 39. NTSB RAR-19-02, Ariel View	52
Figure 40. NTSB RAR-19-02, Overview Resting Position.....	52
Figure 41. NTSB RAR-19-02, Overview	53
Figure 42. NTSB RAR-19-02, Front Locomotive	53
Figure 43. NTSB RAR-16-03, Overview	54
Figure 44. NTSB RAR-16-03, Southbound Locomotive	55
Figure 45. NTSB RAR-15-02, Overview Resting Position.....	56
Figure 46. NTSB RAR-15-02, Overview	56
Figure 47. NTSB RAR-15-02, Close-up View.....	57
Figure 48. SD70MAC Locomotive FE Model	58
Figure 49. Actual Locomotive for Comparison (Wikimedia Commons).....	59
Figure 50. NTSB RAR-21-01 BNSF Railroad Collision Near Kingman, AZ, Overview (Source: Oklahoman.com).....	59
Figure 51. Ship Car FE Model.....	60
Figure 52. Actual Ship Car for Comparison, Overview (Source: Wikipedia).....	60
Figure 53. FE Model of the Auto-Rack Car	61
Figure 54. Actual Auto-Rack Car for Comparison (Source: Wordpress/lionel-llc).....	61
Figure 55. NTSB RAR 13-02 Eastbound UPRC Freight Train, Close-up	62
Figure 56. NTSB RAR 13-02 Eastbound UPRC Freight Train, Overview	62
Figure 57. NTSB RAR 13-02 Westbound UPRC Freight Train, Close-up.....	62
Figure 58. NTSB RAR 13-02 Westbound UPRC Freight Train, Overview.....	62
Figure 59. NTSB RAR 13-02 Eastbound and Westbound UPRC Freight Trains at Impact, Close- up.....	63

Figure 60. NTSB RAR 13-02 Eastbound and Westbound UPRC Freight Trains at Impact, Overview.....	63
Figure 61. NTSB RAR 13-02 Eastbound and Westbound UPRC Freight Trains at Impact, Overview.....	63
Figure 62. FE Simulation Results, 0 second.....	64
Figure 63. FE Simulation Results, 1 second.....	64
Figure 64. FE Simulation Results, 2 seconds.....	64
Figure 65. FE Simulation Results, 3 seconds.....	65
Figure 66. FE Simulation Results, 4 seconds.....	65
Figure 67. FE Simulation Results, 5 seconds.....	65
Figure 68. FE Simulation Results, 6 seconds.....	66
Figure 69. FE Simulation Results, 7 seconds.....	66
Figure 70. FE Simulation Results, 8 seconds.....	66
Figure 71. FE Simulation Results, 9 seconds.....	67
Figure 72. FE Simulation Results, 10 seconds.....	67
Figure 73. FE Simulation Results, 11 seconds.....	67
Figure 74. FE Simulation Results, 12 seconds.....	68
Figure 75. FE Simulation Results, 13 seconds.....	68
Figure 76. FE Simulation Results, 14 seconds.....	68
Figure 77. FE Simulation Results, 15 seconds.....	69
Figure 78. NTSB RAR 13-02 Post-Impact Comparison Between the Crash and Simulation, Close-Up of Crash.....	69
Figure 79. NTSB RAR 13-02 Post-impact Comparison Between the Crash and Simulation, Close-Up Simulation.....	70
Figure 80. NTSB RAR 13-02 Post-impact Comparison Between the Crash and Simulation, Close-Up of Crash.....	70
Figure 81. NTSB RAR 13-02 Post-impact Comparison Between the Crash and Simulation, Close-Up Simulation.....	71
Figure 82. NTSB RAR 13-02 Post-impact Comparison Between the Crash and Simulation, Close-Up of Crash.....	71
Figure 83. NTSB RAR 13-02 Post-impact Comparison Between the Crash and Simulation, Close-Up Simulation.....	72
Figure 84. NTSB RAR 13-02 Post-Impact Comparison Between the Crash and Simulation, Close-Up of Crash (newschannel10.com).....	72
Figure 85. NTSB RAR 13-02 Post-Impact Comparison Between the Crash (Source fom newschannel10.com) and Simulation, Close-up.....	73

Figure 86. Simulation Energies.....	73
Figure 87. Original Model Set-up (From Test 6 Report).....	74
Figure 88. Test 6 Pre-Impact Comparison.....	75
Figure 89. Test 6 Pre-Impact Comparison.....	75
Figure 90. Test 6 Pre-Impact Comparison.....	76
Figure 91. Sequential Images between Simulation and TTC Crash Test, Top View at 100 ms...	76
Figure 92. Sequential Images between Simulation and TTC Crash Test, Top View at 200 ms...	77
Figure 93. Sequential Images between Simulation and TTC Crash Test, Top View at 300 ms...	77
Figure 94. Sequential Images between Simulation and TTC Crash Test, Front View at 100 ms	78
Figure 95. Sequential Images between Simulation and TTC Crash Test, Front View at 200 ms	78
Figure 96. Sequential Images between Simulation and TTC Crash Test, Front View at 300 ms	78
Figure 97. Sequential Images between Simulation and TTC Crash Test, Front View at 400 ms	78
Figure 98. Sequential Images between Simulation and TTC Crash Test, Rear View at 100 ms .	79
Figure 99. Sequential Images between Simulation and TTC Crash Test, Rear View at 200 ms .	79
Figure 100. Sequential Images between Simulation and TTC Crash Test, Rear View at 300 ms	79
Figure 101. Sequential Images between Simulation and TTC Crash Test, Rear View at 400 ms	80
Figure 102. Post-Impact Crush Comparison.....	80
Figure 103. Post-Impact Crush Comparison.....	81
Figure 104. Post-Impact Crush Comparison.....	81
Figure 105. Simulation Energies.....	81
Figure 106. S-580: 750,000/500,000 Collision Post Loading	82
Figure 107. S-580: Cylindrical Shape of 126 in (length) at 30 mph.....	83
Figure 108. S-580: Cylindrical Shape Simulation Sequential Images at 0 ms	83
Figure 109. S-580: Cylindrical Shape Simulation Sequential Images at 150 ms	84
Figure 110. S-580: Cylindrical Shape Simulation Sequential Images at 200 ms	84
Figure 111. S-580: Cylindrical Shape Simulation Sequential Images at 250 ms	84
Figure 112. S-580: Rectangular Shape Offset by 12 in at 30 mph	85
Figure 113. S-580: Rectangular Shape Simulation Sequential Images at 0 ms.....	85
Figure 114. S-580: Rectangular Shape Simulation Sequential Images at 100 ms.....	85
Figure 115. S-580: Rectangular Shape Simulation Sequential Images at 220 ms.....	86
Figure 116. S-580: Rectangular Shape Simulation Sequential Images at 420 ms.....	86
Figure 117. S-580: 500,000/200,000 Collision Post Loading for Previous Locomotive Regulations	87

Figure 118. S-580: Cylindrical Shape Simulation Sequential Images for non-modern Locomotive Regulations at 0 ms.....	88
Figure 119. S-580: Cylindrical Shape Simulation Sequential Images for non-modern Locomotive Regulations at 150 ms.....	88
Figure 120. S-580: Cylindrical Shape Simulation Sequential Images for non-modern Locomotive Regulations at 200 ms.....	89
Figure 121. S-580: Cylindrical Shape Simulation Sequential Images for non-modern Locomotive Regulations at 250 ms.....	89

Executive Summary

On January 1, 2009, the Federal Railroad Administration (FRA) Final Rule of compliance with the 49 Code of Federal Regulations (CFR) Part 229 and Part 238 standards went into effect. All locomotives manufactured or remanufactured since then must be compliant with the new crashworthiness standards, as well as the Association of American Railroads' (AAR) S-580-2005 crashworthiness requirements. Locomotives are mandated by the FRA Final Rule to be compliant with the 49 Code of Federal Regulations (CFR) Part 229 and Part 238 standards as well as AAR's S-580-2005 crashworthiness requirements. Locomotives manufactured or remanufactured after 2009 are considered "modern", and those manufactured before 2009 are considered "not modern" in this study.

The FRA Accident and Incident Database and National Transportation Safety Board (NTSB) Accident and Incident Database (referred to as the FRA and NTSB accident databases) identify six freight train collisions and derailments involving modern locomotives that resulted in-cab occupant casualties. There are several possible reasons why these casualties occurred in spite of the improved crashworthiness of modern locomotives. Train lengths have steadily increased over time, (some trains are now over 11,000 ft) with larger freight capacity (over 12,500 tons). In addition, operation speeds have increased in some rail sections across the country. In the event of a collision, the greater magnitude of impact force from a heavier/faster train could exceed the design crashworthiness requirements of the struck locomotive. Hence, to improve rail safety and enhance railroad operational efficiency, the adequacy of modern locomotive crashworthiness should be reevaluated vis-à-vis the established AAR S-580 requirements.

This project aims to fulfill these research needs, and builds upon decades of similar research by FRA, NTSB, and AAR. The project's objective was to evaluate the effects of the AAR S-580 requirements for modern locomotive crashworthiness through a combination of statistical analysis and finite element (FE) modeling and simulations. The research team evaluated modern locomotive structural features to ascertain their stated crashworthiness and structural integrity. They also analyzed current locomotive FE model(s) and executed an upgrade plan. Rigorous validations with the complied data provided confidence that the upgraded FE model(s) are viable in predicting a freight train response in crashes. The team divided the project into six tasks. For Task 1, the team surveyed the FRA and NTSB accident databases to identify major revenue service freight train collision cases. For Task 2, the team developed collision evaluation criteria to aid in the assessment of the need for further improvements to the crashworthiness requirements as specified in AAR S-580.

For Task 3, the team reviewed available crash tests and FE models to pick a case to validate the FE model. Then, the model went through vigorous upgrades based on remeshing, materials, properties, connections, and constrained levels to meet current industry standards. The model also received a geometric upgrade to match the exact shape of the crash test train car. For Task 4, the simulation was set up and conducted. Many iterations were performed to meet the industry level of validation. Based on the similar behavior of the locomotive and hopper car crush and the comparison between the simulation and the crash test data, the model was deemed validated.

For Task 5, the research team simulated the collision cases from the collision evaluation criteria in Task 2. The simulated collisions were examined to confirm the crashworthiness, including the cab crew safety of the modern locomotives.

For Task 6, the researchers validated an additional crash test to thoroughly evaluate the front-end structure and the safety of the locomotive cab. Then, the team simulated the recommended regulation scenarios and thoroughly assessed the crashworthiness of the cab and safety of the crew in modern locomotives.

The research team developed a proven, high-fidelity locomotive FE model with improved collision evaluation criteria. Upon successful completion, the modern freight locomotive's crashworthiness and its compliance with AAR S-580 requirements were analyzed and evaluated, considering the effect of freight train collisions on crew safety and revenue. The long-term benefits of this project are expected to be improvements in freight railroad operational efficiency and safety of modern locomotive cab crew in the event of a collision.

1. Introduction

1.1 Background

The U.S. freight railroad industry has built a commendable reputation as one of the safest in the world. It is also the largest in terms of the total annual ton-miles of freight transported, and accounts for nearly 28 percent of all the goods transported across the continental U.S. Even with the railroad industry's safety-conscious actions, it is possible that the impact forces of a collision could exceed the design crashworthiness requirements of the locomotive. Hence, to further improve rail safety and to enhance railroad operational efficiency, the adequacy of modern locomotive crashworthiness should be evaluated vis-à-vis the established requirements.

The Federal Railroad Administration (FRA) Office of Research, Development, and Technology (RD&T) has been conducting research on locomotive crashworthiness since the mid-1980s. Additionally, the National Transportation Safety Board (NTSB) has been investigating all major rail collision and derailment cases involving crew casualties since the 1970s. This work led to their recommendations to enhance the locomotive crashworthiness. These recommendations also motivated the Association of American Railroads (AAR) to conduct research aimed at improving the safety of the cab crew in the event of revenue service accidents.

In 1989, the AAR adopted the Locomotive Crashworthiness standard S-580. In March 1996, FRA established the Railroad Safety Advisory Committee (RSAC) which provided a forum for consensual rulemaking and program development. FRA worked towards the development of the Locomotive Crashworthiness Regulations, using the recommendations made by an FRA-led government/industry committee and the RSAC. FRA's Locomotive Crashworthiness Final Rule was published on June 28, 2006 under the Title 49 CFR Part 229 and 49 CFR Part 238, which became effective on August 28, 2006. Appendix E to 49 CFR Part 229 specifies the performance criteria for locomotive crashworthiness.

Based on further research and analyses including the RSAC recommendations, AAR produced the S-580 in 2005, including crashworthiness requirements effective January 2009. This standard also includes requirements for applied force/strength of the locomotive forebody components (e.g., the anti-climber, collision posts, short hood, cabin window frame, underframe, fuel tank, and truck attachment.) Since 2005, AAR has revised and updated the standard; however, the technical specifications of the crashworthiness requirements remained essentially the same from the 2005 revision (The Association of American Railroads, 2020).

All freight locomotives manufactured or remanufactured after January 1, 2009 are recognized as "modern locomotives." FRA mandated their compliance with the crashworthiness standards defined in Subpart D of 49 CFR Part 229 and in the applicable AAR S-580 locomotive crashworthiness requirements (U.S. Federal Railroad Administration, 2006). Locomotives manufactured or remanufactured before 2009 are labeled as "not-modern locomotives" throughout this report and future reports of this project.

1.2 Objective

This project's objective was to evaluate the effects of the AAR S-580 requirements for modern locomotive crashworthiness through a combination of statistical analysis and finite element (FE) modeling and simulations. Modern locomotive structural features were evaluated to ascertain their stated crashworthiness and structural integrity. As part of this effort, the team evaluated the

current locomotive FE model(s) and executed an upgrade plan. Rigorous validations with the compiled data provided confidence that the upgraded FE model(s) are viable in predicting a freight train response in crashes.

The research team made recommendations for further revisions to the technical specifications of AAR S-580 crashworthiness requirements, including potential strengthening or modification of vulnerable components without adequate structural strength/stiffness. The team also developed a proven high-fidelity locomotive FE model along with improved collision evaluation criteria. Upon successful completion, the modern freight locomotive's crashworthiness and its compliance with AAR S-580 requirements were analyzed and evaluated considering the importance of freight train collisions on crew safety and revenue. The long-term benefits of this project are expected to be improvements in freight railroad operational efficiency and safety of modern locomotive cab crew in the event of a collision.

The research team divided the project into six tasks. The objective of Task 1 was to review FRA and NTSB accident investigation databases to identify major freight train accident cases involving modern locomotives. The list of accidents compiled in Task 1 identifies important crash-related parameters (collision types, closing speed at impact, crew casualties, road locomotive numbers involved in the collisions, etc.) Using the available data, (i.e., manufacture year and model number) modern locomotives were verified against the rosters of specific railroads.

The objective of Task 2 was to develop appropriate freight railroad collision evaluation criteria to help assess modern locomotive's design crashworthiness adequacy (per AAR S-580) in ensuring cabin crew safety in the event of severe collisions during routine revenue service.

The objectives of Tasks 3 and 4 were to review the available FE models, perform an FE upgrade, and then use the upgrade in the validation process for a crash test. The outcomes of these tasks were used in conducting specific collision simulation studies under Task 5. The collision cases used in Task 5 were chosen from the collision evaluation criteria from Task 2 (retrieved from the NTSB railroad accident investigation database). The simulated collisions were examined with the objective of ascertaining the crashworthiness including the cab crew safety of the modern locomotives.

The objective of Task 6 was to evaluate the impact of the S-580 regulations on the crashworthiness of modern locomotives by assessing the performance of the front-end structure when proxy objects impacted the locomotive. The FE model was revised to provide additional validation of the locomotive cab, utilizing an available TTC crash test. The revised FE model was used to analyze the allowable intrusions into the locomotive hood and cab limits, which was crucial in evaluating the effect of the S-580 regulations on modern locomotives.

1.3 Overall Approach

The research team reviewed the FRA and NTSB accident databases. Based on this review, they developed collision evaluation criteria to aid in the assessment of current locomotive crashworthiness requirements and to suggest future revisions of these requirements. The team also reviewed the available FE models, which were validated using the identified key tests and collisions to provide confidence in replicating freight train crashes. Using one or more of the identified critical collisions and the validated FE model(s), the research team conducted specific collision simulation studies to evaluate the crashworthiness of modern locomotives. They

analyzed the simulation results to produce a summary of the critical observations and an assessment of the impact of AAR S-580 requirements towards ensuring the crashworthiness of modern locomotives. These observations and assessments may be used to execute an upgrade plan as necessary.

Of the 22 major freight railroad accident cases since 2009, (gleaned from the NTSB railroad accident investigation database in Task 1) only six cases involved modern locomotives in the lead of the train consist. The research team analyzed post-accident casualties and estimated damages, and determined that not all collisions involving modern locomotives were severe enough to warrant an evaluation of the concerned locomotive crashworthiness design requirements beyond the approved standard. Therefore, they adopted a two-step approach to develop the modern locomotive collision evaluation criteria. In step 1, the team used a novel combination of a ranking metric and weighting factor to create a shortlist of accident cases based on their collision severities. In step 2, the shortlisted cases and more severe accident cases were analyzed to select the critical locomotive collision parameters which contributed to the collision evaluation criteria.

Next, the FE models were upgraded based on their mesh quality, materials, properties, connections, and their geometric shapes in order to capture the test cars. Thereafter, the model was set up exactly like the TTC test and simulations were performed. After many iterations, the simulation captured the test kinematics, and the model was deemed validated. The team observed that the crash reports focused on the pre-impact phase of the crash and not the post-impact phase. The reports also centered on human factors (e.g., health, schedule, training, rail equipment, etc.) and did not address the locomotives/train cars crashworthiness factors. Based on the findings in the NTSB reports, the researchers revised the FE models and the validation from Tasks 3 and 4 to better simulate the selected collision cases. This revision was considered crucial since the team had limited access to NTSB crash data related to the post-crash information and because of the team's intent to achieve the research project goals.

Once the FE models were revised, the team set up the NTSB selected collision cases from Task 2. Each case had similar train cars, exact weight, speed, initial impact location, similar track elevation, and curvature. The models were simulated and the results were compared with the available data. The team had reviewed the remaining available TTC crash tests that had been performed over the years (some team members were involved in this testing). They selected a moderate locomotive intrusion as the desired crash scenario to simulate and capture frontal intrusions. They found TTC crash Test 6 to be a suitable crash scenario.

After validating the FE model, the team investigated whether the current model locomotive met the dynamic requirements of the S-580 regulations. They considered two dynamic collision scenarios for the evaluation. The first scenario involves a cylindrical-shaped proxy object, weighing at least 65,000 lbs, impacting the locomotive head-on at a speed of 30 mph. The second scenario involves a block-shaped proxy object, also weighing at least 65,000 lbs, impacting the locomotive at 30 mph with a 12 in overlap.

Once the FE models were updated to reflect the selected scenarios, the team conducted simulations to assess the static loading and ensure that the collision posts meet the necessary requirements. Furthermore, the team addressed the overall comparison between the latest regulation (S-580) and the previous S-580 regulation prior to 2005. This comparison aimed to evaluate the impact of the latest regulation on the crashworthiness of modern locomotives.

1.4 Organization of the Report

Section 2 outlines Task 1, which consisted of searching the freight train accident databases using the established criteria, generating an initial list of major accidents and incidents for this project, and reviewing the reports and data from the initial list.

Section 3 covers Task 2, in which the team proposed a ranking metric for the more severe modern locomotive collisions to help refine collision evaluation criteria. This metric considered multiple operational parameters, including the type of collision (e.g., head-on, rear-end), the closing speed at the point of impact, and crew casualties.

Section 4 covers Tasks 3 and 4, which aimed to identify and validate the FE models, including reviewing the FE models, crash test analysis, reviewing the challenges faced, a visit to the train yard, online research, and upgrading the validated FE models.

Section 5 discusses Task 5's aim to conduct specific collision simulations of the top selected cases identified in Task 2. The team conducted a comprehensive review of the NTSB's most significant crash cases and made updates to the current FE models while also designing new models for the train cars that were missing. All simulations were performed using the renown FE code (LS-DYNA), and run for a duration of 20 seconds. The train derailments observed during the simulation demonstrated a satisfactory resemblance to the actual crash site.

Section 6 outlines Task 6, in which the team made additional improvements to the FE model and evaluated the latest S-580 regulations, with a focus on two key elements: the dynamic aspect and the quasi-static loads of the collision posts, since they directly relate to the locomotive cab intrusion. The FE simulations were then conducted based on the setup described in the previous section and previous TTC tests. The research team found a remarkable similarity in behavior between the locomotive and the elevated intermodal container in both the simulation and the crash test impact.

Section 7 presents the conclusion of the research results. These results demonstrate that modern locomotives, designed in accordance with the updated S-580 regulations, offer improved safety compared to older locomotives. The modern designs provide better protection for the crew during crashes, enhancing their overall safety and minimizing the risk of injuries.

2. Task 1

2.1 Task 1 Research Methodology

For Task 1, the team reviewed the project objectives and established a plan to direct their efforts. This plan included:

- Identify and define the criteria to sort and filter the freight train accident databases.
- Search the freight train accident databases using the established criteria.
- Generate an initial list of major accidents and incidents relevant for this project.
- Compile and review the relevant reports and available data from the initial list.

The team analyzed the freight railroad locomotive fleet records and found that modern locomotives constituted a small fraction of the total road locomotives in the inventory of Class I railroads, from 2 percent in 2009 to 21 percent in 2019 (U.S. Department of Transportation, 2020). [Figure 1](#) depicts the locomotive fleet size from 1990 to 2019, showing the number of modern locomotives relative to the non-modern locomotives after 2009, when the AAR S-580-2005 crashworthiness requirements were mandated.

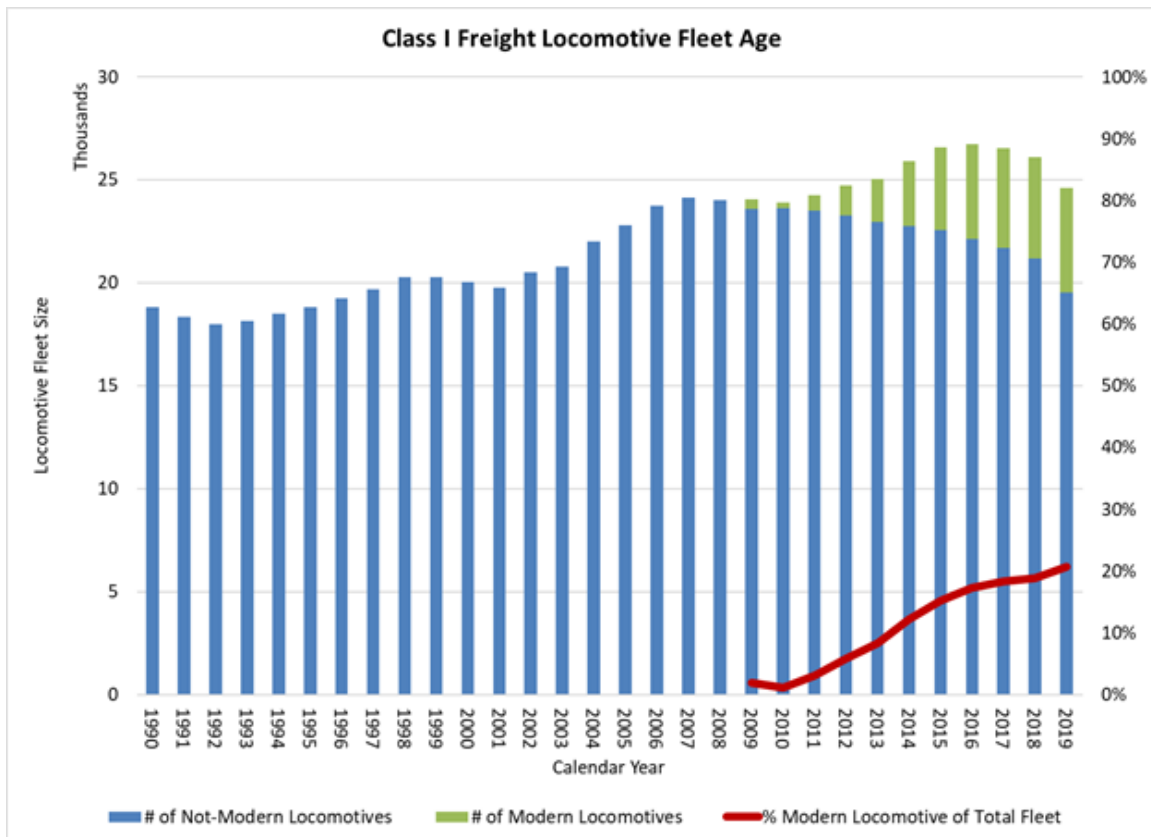


Figure 1. Class I Freight Locomotive Ratio of Modern to Non-Modern Locomotives

[Figure 2](#) depicts the variation of accident/incident rates of U.S. Class I freight railroads throughout the decade after modern locomotives were introduced.

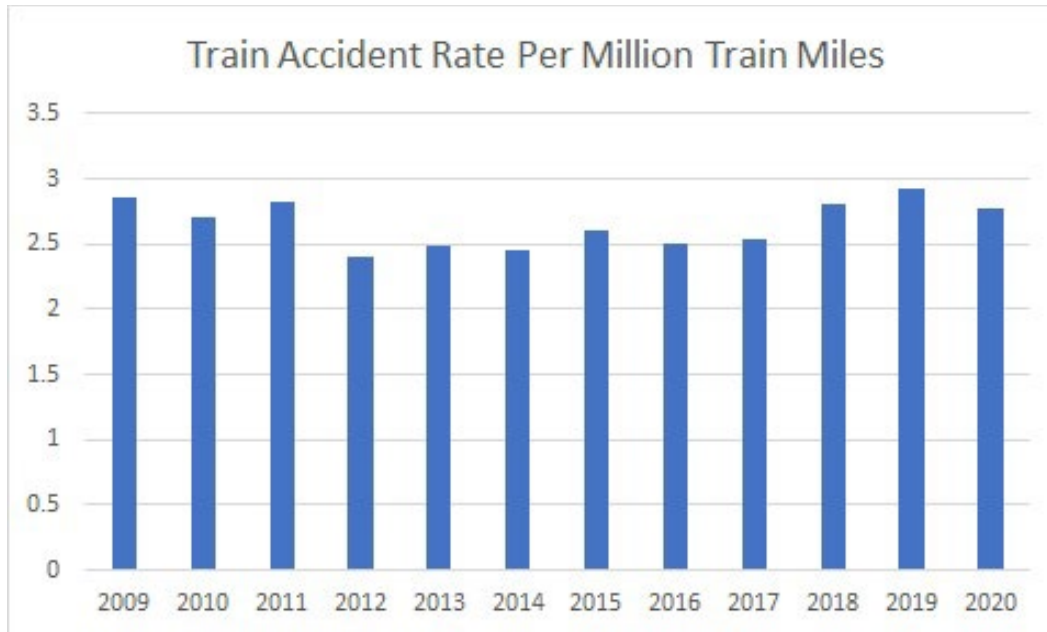


Figure 2. Accident/Incident Rates per Class I Freight Million Miles (U.S. Federal Railroad Administration, 2021)

Figure 3 shows the trend in post-accident in-cab casualties since the introduction of modern locomotives, with a decreasing number of casualties in the second half of the decade.

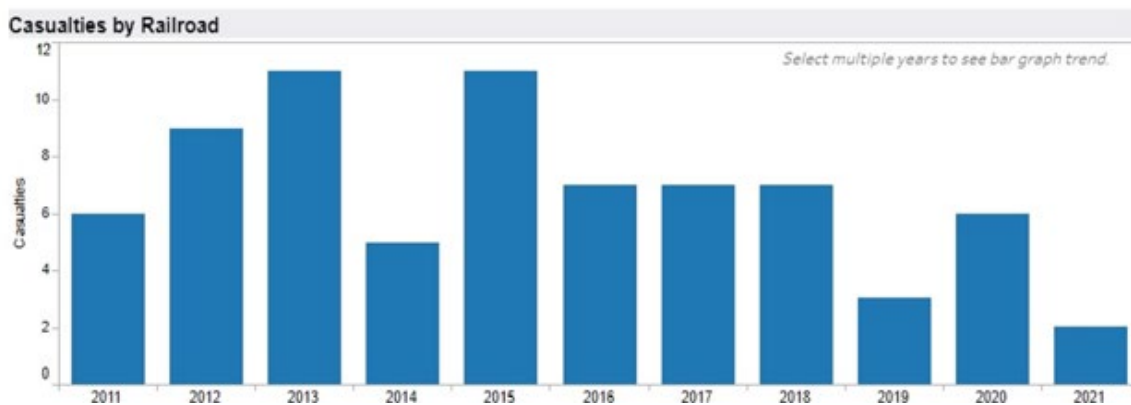


Figure 3: Number of Post-Accident In-cab Casualties of U.S. Class I Freight Railroads in Revenue Service (U.S. Federal Railroad Administration, 2021)

No clear trend was identified from the information in these figures, in either the accident/incident rates per class I freight million miles or the number of post-accident in-cab casualties of class I railroads in revenue service following the introduction of modern locomotives. The research team decided to perform another database search, this time including all major freight train accident investigation cases post-2009. This bolstered the search criteria to identify the collision cases that involved modern locomotives. The search criteria filtered for accident investigation reports adopted in 2009 or more recently, involving revenue service freight trains, and involving at least one road locomotive (as opposed to yard or switch locomotives).

After refining the search scope, the team surveyed the NTSB Railroad Accident Reports database (U.S. National Transportation Safety Board, 2021) and NTIS Reports database (National

Technical Information Service, 2021) for appropriate freight train collision cases. The search focused on freight locomotive accidents and incidents with the potential to support FE modeling and crashworthiness simulations in future Tasks.

Next, the researchers collected the accident preliminary reports and corresponding docket documents containing detailed investigation data for each identified collision case (e.g., train details, closing speed at the time of impact, locomotive crew fatality/injury, and associated NTSB and NTIS report numbers). They cross-referenced road locomotive numbers from the reports with the corresponding railroad locomotive roster (Craig, 2021) to determine the year of manufacture (or last remanufacture) to ascertain if it was a modern locomotive with full compliance with the AAR S-580 crashworthiness requirements.

These tabulated data served in the development of the collision evaluation criteria in Task 2 and in the selection of collision cases to be used in FE modeling and collision simulations in subsequent Tasks. The primary goal of the project is to evaluate the crashworthiness performance of the concerned modern locomotives involved in the selected revenue service accident scenarios towards confirming their compliance with the AAR S-580 crashworthiness requirements.

2.2 Accident and Collision Data

2.2.1 Data Summary

The team identified 22 major accident cases in the databases. Some accident cases involved multiple collisions, such as when a collision resulted in locomotives and/or cars fouling an adjacent track, which were then struck by a passing train. Tables are distinguished by “accidents”, which are linked to a single NTSB case and “collisions” to identify all trains involved in the accidents.

2.2.2 Identified Accidents

Table 1 lists the cases in chronological order, starting with the most recently released report. This table provides all relevant information about the reports.

Table 1. Accidents Identified from Databases Surveys

NTSB Report Number	NTSB Report Adoption Date	NTSB Docket Number	NTIS Accession Number	Collision Date	Collision Location
RAR-21-01	05/10/2021	RRD18FR009	N/A	06/05/2018	Kingman, AZ
RAR-20-05	12/21/2020	RRD19FR001	PB2020-101016	10/04/2018	Granite Canyon, WY
RAR-20-03	08/12/2019	RRD19FR010	PB2020-101009	08/12/2019	Carey, OH
RAR-19-02	07/23/2019	RRD18MR003	PB2019-101308	02/04/2018	Cayce, SC
RAB-19-02	06/11/2019	DCA16FR008	N/A	06/28/2016	Panhandle, TX
RAB-17-10	12/01/2017	DCA16MR005	N/A	03/14/2016	Granger, WY
RAB-17-08	10/12/2017	DCA15FR014	N/A	09/08/2015	Texarkana, TX
RAB-17-01	02/07/2017	DCA14MR004	N/A	12/30/2013	Casselton, ND
RAR-16-03	12/19/2016	DCA14FR011	PB2017-100970	08/17/2014	Hoxie, AR
RAB-15-08	12/09/2015	DCA14FR012	N/A	09/25/2014	Galva, KS
RAR-15-02	06/25/2015	DCA13FR013	PB2015-105169	09/25/2013	Amarillo, TX

NTSB Report Number	NTSB Report Adoption Date	NTSB Docket Number	NTIS Accession Number	Collision Date	Collision Location
RAB-15-04	04/14/2015	DCA13FR008	N/A	07/16/2013	Hays, KS
RAB-14-14	12/01/2014	DCA14FR003	N/A	12/30/2013	Keithville, LA
RAR-14-02	11/17/2014	DCA13MR004	PB2015-102084	05/25/2013	Chaffee, MO
RAB-14-05	07/03/2014	DCA12FR007	N/A	07/21/2012	Barton County, MO
RAB-13-03	08/20/2013	DCA12FR002	N/A	01/06/2012	Westville, IN
RAR-13-02	06/18/2013	DCA12MR005	PB2013-107679	06/24/2012	Goodwell, OK
RAR-13-01	02/12/2013	DCA10FR009	PB2013-104865	09/30/2010	Two Harbors, MN
RAB-13-01	01/29/2013	DCA11FR004	N/A	05/24/2011	Mineral Springs, NC
RAR-12-02	04/24/2012	DCA11FR002	PB2012-916302	04/17/2011	Red Oak IA
RAB-12-02	03/29/2012	DCA11FR001	N/A	03/23/2011	Kelso, WA
RAR-10-01	01/21/2010	DCA08MR009	PB2010-916301	03/12/2008	Chatsworth, CA

2.2.3 Summaries of Identified Collisions

Table 2 summarizes each collision rather than each NTSB case, as some accidents resulted in more than one train collision. The 22 accident cases resulted in 24 collisions. To identify each collision, the NTSB report number was repeated with an appended indicator (i.e., 1 or 2) to chronologically identify the collisions. A short description and/or probable cause(s) provide a basic understanding of the collisions.

The types of collisions are divided into the following impact categories:

- Head-on: 8 cases.
- Rear-end: 6 cases, 2 cases also collided with on-track equipment such as Maintenance of Way (MOW) trains.
- Oblique/Raking: 5 cases.
- Collisions with stationary or derailed cars, or on-track equipment: 6 cases, 2 cases also included rear-end collisions.
- Highway-rail grade crossings: 1 case.

Table 2. Descriptions of Collisions

NTSB Report Number	Description/ Probable Cause	Striking Train ID	Striking Train Type	Struck Train ID	Struck Train Type	Impact Category
RAR-21-01	Crew of striking train exceeded restricted speed requirements and could not stop in time.	BNSF S MEMSCO1 02L	Intermodal-Freight	WNEESGM 1 05	MOW	Rear end with on-track equipment
RAR-20-05	Striking train's brake failure led to uncontrollable run away.	UP MGRCY04	Freight	UP MPCNP03	Freight	Rear end
RAR-20-03	Engineer of striking train did not follow signals due to alcohol impairment.	CSX H70211	Freight	CSX W31411	Freight	Oblique/Raking

NTSB Report Number	Description/ Probable Cause	Striking Train ID	Striking Train Type	Struck Train ID	Struck Train Type	Impact Category
RAR-19-02	Conductor of struck train failed to properly reposition switch and CSX signal system suspended without backup.	Amtrak P91	Passenger	CSX F777	Freight	Head-on
RAB-19-02	Crew of striking train did not follow signals.	BNSF S LACLPC1-26K	Intermodal - Freight	BNSF Q CHISBD6 27L	Intermodal-Freight	Head-on
RAB-17-10	Signal system suspended and employee in charge misunderstood dispatcher and authorized striking train movement with switch misaligned.	UP KG1LAC-13	Intermodal - Freight	UP LCK41-14	Coal - Freight	Head-on
RAB-17-08	Crew of striking train did not follow signals and entered occupied grade crossing.	UP AMNML-07	Auto rack - Freight	UP ALDAS-06	Freight	Oblique/Raking
RAB-17-01	Before accident, struck train car derailed and fouled adjacent track. Striking train collided with grain car.	BNSF G-RYLRGT9-26A	Tanker - Freight	Derailed railcar from BNSF U-FYNHAY4-05	Grain - Freight	Collision with on-track derailed cars
RAR-16-03	Single main track transition to double main track and crew of striking train did not follow signals due to fatigue.	UP IMASNL-16	Freight	UP IQNLPI-17	Freight	Head-on
RAB1508	Signals were not clear and crew of striking train passed red signal and entered siding raking struck train.	UP ILXG4X-22	Intermodal - Freight	UP KG4GSX-23	Intermodal - Freight	Oblique/Raking
RAR-15-02 (#1)	Red signal light not working/illuminated at night and crew of striking train did not notice with freight cars derailling and fouled adjacent track.	BNSF BLACWSP2 23A	Freight	BNSF SLHTLPC2 23A	Freight	Rear-end
RAR-15-02 (#2)	Striking train hit derailed trains cars fouling track from collision immediately before.	BNSF ZWSPSBD72 4L	Intermodal - Freight	N/A	Derailed Freight cars	Collision with on-track derailed cars
RAB-15-04	Hand-operated switch misassigned and directed striking train off main track on to siding track.	UP MSIDV 16	Freight	N/A	Stationary Freight cars	Collision with on-track stationary cars
RAB-14-14	Hand-operated switch misaligned and directed striking train off main track on to siding track.	UP MPBSR 30	Freight	BNSF E MLMNAM 0 16, (UP designation CMRNAJ 23)	Coal - Freight	Head-on

NTSB Report Number	Description/ Probable Cause	Striking Train ID	Striking Train Type	Struck Train ID	Struck Train Type	Impact Category
RAR-14-02	Engineer of striking train did not follow signals and speed restrictions and entered occupied grade crossing.	UP 2-ASMAR-25	Freight	BNSF U-KCKHKM0-05T	Freight	Oblique/Raking
RAB-14-05	Crew of striking train did not follow signals and speed restrictions and entered occupied grade crossing.	KCS QSHKC20	Freight	BNSF EMHSEBM 088	Freight	Oblique/Raking
RAB-13-03 (#1)	Engineer of striking train did not follow signals and rear-ended stationary train with the lead locomotive of striking train falling on its side, fouling the adjacent track.	CSX Q39506	Freight	CSX K68303	Tanker - Freight	Rear-end
RAB-13-03 (#2)	Striking train hit derailed locomotive from collision immediately before.	CSX Q16105	Intermodal Freight	N/A	Derailed locomotive and freight cars from adjacent track	Collision with on-track derailed locomotive
RAR-13-02	Engineer of striking train did not follow signals because of deteriorating vision.	UP ZLAAH-22	Freight	UP AAMMLX-22	Freight	Head-on
RAR-13-01	Engineer of striking train did not follow authority instructions and entered main track from siding.	CN U78982-30	Ore - Freight	CN U78983-30	Ore - Freight	Head-on
RAB-13-01	Crew of striking train did not follow signals and speed restrictions.	CSX Q19423	Freight	CSX Q61822	Freight	Rear-end
RAR-12-02	Crew of striking train did not follow signals and speed restrictions due to fatigue and lead locomotive modular cab detached from underframe.	BNSF C-BTMCNM0-26	Coal - Freight	BNSF U-BRGCRI-15	MOW	Rear end with on-track equipment
RAB-12-02	Passenger motor vehicle entered grade crossing in front of striking train.	BNSF G-CRKINB9-16H	Grain/Hopper - Freight	N/A	Passenger motor vehicle	Highway-rail grade crossing
RAR-10-01	Engineer of striking train did not follow signals and speed restrictions due to distraction from text messaging.	Southern California Metrolink 111	City Metro Passenger	UP LOF65-12	Freight	Head-on

2.2.4 Severity Parameters of Identified Accidents

Table 3 shows the severity parameters of each accident. Note that the outcomes from all collisions within an accident case are combined and presented as one summary for each NTSB report.

Table 3. Accident Severity Parameters

NTSB Report Number	Crew Fatalities	Crew Injuries	Non-Crew Fatalities and/or Serious Injuries	Closing Speed (MPH)	Estimated Damage Cost (\$ Millions)
RAR-21-01	1	1	0	14	1.0
RAR-20-05	2	0	0	55	3.2
RAR-20-03	0	0	0	Striking 10 and Struck 25	4.5
RAR-19-02	2	0	92	50	25.4
RAB-19-02	3	0	0	94	16
RAB-17-10	0	1	0	30	N/A
RAB-17-08	0	0	0	6	4.7
RAB-17-01	0	0	0	44	13.5
RAR-16-03	2	0	0	80	10.7
RAB-15-08	0	2	0	47	3.2
RAR-15-02	0	5	0	25	4.4
RAB-15-04	0	3	0	49	1.4
RAB-14-14	0	4	0	34	7.8
RAR-14-02	0	2	0	43	11
RAB-14-05	0	2	0	31	7.8
RAB-13-03	0	2	0	Rear end 35	5
RAR-13-02	2	0	0	97	14.8
RAR-13-01	0	5	0	54	8.1
RAB-13-01	2	2	0	48	1.6
RAR-12-02	2	0	0	23	8.7
RAB-12-02	0	0	2	47	0.032
RAR-10-01	0	0	126	84	12

2.2.5 Lead Locomotives Involved in Collisions

Table 4 catalogs the striking train’s lead locomotive as identified in the FRA and NTSB accident databases. Table 5 catalogs the corresponding struck lead locomotives. Some struck trains/train cars did not have locomotives or locomotives were not involved in the accidents (noted as N/A). In addition, the docket documents of some accidents were not released or the available data did not provide enough information to identify the lead locomotives (noted as Not specified). Records of the locomotive manufacture year or year of last remanufacture were collected from *The Diesel Shop’s Locomotive Roster* (Craig, 2021) to determine if the lead locomotive is modern. Retired locomotives were permanently removed from service as a result of the collision; locomotives actively used in freight revenue trains in 2021 are considered in service. Missing or inconclusive data are recorded as Unknown. The information collected in this Task will be further analyzed in Task 2 to develop collision evaluation criteria.

Table 4. Striking Train's Lead Locomotive

NTSB Report Number	Locomotive Road ID	Make	Model	Year of Manufacture /Remanufacture	Modern?	Disposition
RAR-21-01	BNSF 4283	GE	ES44C4	2016	Yes	In service
RAR-20-05	UP 5412	GE	ES44AC	2005	No	Retired
RAR-20-03	CSXT 736	GE	ES44AC-H	2007	No	Unknown
RAR-19-02	AMT 47	GE	P42DC	1997	No	Retired
RAB-19-02	BNSF 5162	GE	C44-9W	2004	No	Retired
RAB-17-10	UP 5718	GE	AC44CWCTE	2001	No	Unknown
RAB-17-08	UP 2542	GE	ES44AC	2015	Yes	Retired
RAB-17-01	BNSF 4934	GE	C44-9W	1998	No	Retired
RAR-16-03	UP 9707	GE	C44-9W	1994	No	Retired
RAB-15-08	UP 8572	EMD	SD70ACe	2007	No	In service
RAR-15-02 (#1)	BNSF 7891	GE	ES44DC	2010	Yes	In service
RAR-15-02 (#2)	BNSF 6943	GE	ES44C4	2012	Yes	Retired
RAB-15-04	UP 7276	GE	AC44CW	1999	No	Retired
RAB-14-14	CSXT 5438	GE	ES44DC	2007	No	In service
RAR-14-02	UP 5668	GE	AC44CW-CTE	2004	No	Retired
RAB-14-05	KCSM 4667	GE	ES44AC	2006	No	In service
RAB-13-03 (#1)	CSXT 517	GE	AC44CW	2001	No	Retired
RAB-13-03 (#2)	CSXT 5387	GE	ES40DC	2006	No	In service
RAR-13-02	UP 8542	EMD	SD70ACe	2007	No	Retired
RAR-13-01	IC 6265	EMD	SD40-3	Rebuilt in 2000	No	Retired
RAB-13-01	CSXT 7783	GE	C40-8W	1992	No	Retired
RAR-12-02	BNSF 9159	EMD	SD70ACe	2008	No	In service (Renumbered BNSF 8749)
RAB-12-02	BNSF 7363	GE	ES44DC	2010	Yes	In service
RAR-10-01	SCAX 855	EMD	F59 PH	2001	No	Retired

Table 5. Struck Train's Lead Locomotive

NTSB Report Number	Locomotive Road ID	Make	Model	Year of Manufacture /Remanufacture	Modern?	Disposition
RAR-21-01	N/A	N/A	N/A	N/A	N/A	N/A
RAR-20-05	N/A	N/A	N/A	N/A	N/A	N/A
RAR-20-03	N/A	N/A	N/A	N/A	N/A	N/A
RAR-19-02	CSXT 130	GE	AC44CW	1996	No	Retired
RAB-19-02	N/A	N/A	N/A	N/A	N/A	N/A
RAB-17-10	UP 5155	EMD	SD70M	2004	No	Unknown
RAB-17-08	N/A	N/A	N/A	N/A	N/A	N/A
RAB-17-01	N/A	N/A	N/A	N/A	N/A	N/A
RAR-16-03	N/A	N/A	N/A	N/A	N/A	N/A
RAB-15-08	N/A	N/A	N/A	N/A	N/A	N/A
RAR-15-02 (#1)	BNSF 6781	GE	ES44C4	Unknown	Unknown	In service
RAR-15-02 (#2)	N/A	N/A	N/A	N/A	N/A	N/A

NTSB Report Number	Locomotive Road ID	Make	Model	Year of Manufacture/ Remanufacture	Modern?	Disposition
RAB-15-04	N/A	N/A	N/A	N/A	N/A	N/A
RAB-14-14	BNSF 9735	EMD	SD70MAC	1996	No	Active
RAR-14-02	Not specified	N/A	N/A	N/A	N/A	N/A
RAB-14-05	N/A	N/A	N/A	N/A	N/A	N/A
RAB-13-03 (#1)	CSXT 5387	GE	ES40DC	2006	Unknown	Unknown
RAB-13-03 (#2)	N/A	N/A	N/A	N/A	N/A	N/A
RAR-13-02	UP 8692	EMD	SD70ACe	2011	Yes	Retired
RAR-13-01	IC 6258	EMD	SD40-3	Rebuilt in 1999	No	Retired
RAB-13-01	N/A	N/A	N/A	N/A	N/A	N/A
RAR-12-02	BNSF 9159	EMD	SD70ACe	2007	No	Retired
RAB-12-02	N/A	N/A	N/A	N/A	N/A	N/A
RAR-10-01	UP 8485	EMD	SD70ACe	2006	No	Retired

2.3 Task 1 Conclusions

In this section, 22 freight train accident cases were identified. Summaries included details indicative of accident severity, road locomotive identification, and its year of manufacture or remanufacture. The team has explored finding an easier way to identify freight train accident cases involving only modern locomotives, as the reports presented only the specific road locomotive numbers. The year of manufacture or remanufacture was found by cross-referencing the specific railroad locomotive roster. This work confirmed that there have been only six collisions involving modern locomotives among the identified cases. In Task 2, the team further examined the data compiled in Task 1 and used them to develop appropriate collision evaluation criteria as the next step of the research.

3. Task 2

3.1 Research Methodology

3.1.1 Step 1: Short Listing of More Severe Modern Locomotive Collision Cases

To shortlist (SL) the more severe modern locomotive collision cases, the team used a ranking metric and a weighting factor to identify cases involving modern locomotives in the lead of the colliding freight train consists. The severity of train collisions depends upon operational parameters. These include the type of collision and the magnitude of closing speed at the point of impact between two trains or between one train and stationary rolling stock or on-track equipment.

Crew in-cab casualties are also an important post-collision parameter indicative of the severity of the collision. A very severe collision may result in locomotive crew fatality or fatal injuries, while a less severe collision may cause minor or no crew injury. Similarly, an in-line collision involving a head-on impact between two trains is expected to be much more severe. An in-line rear-end collision is expected to result in a less severe collision, and an oblique or raking collision is expected to be the least severe one. The proposed ranking metric considers the above factors and assigns arbitrary/simple scores corresponding to the grades of severity.

Table 6. Collision Severity Parameters and Scores

Collision Severity Parameter	Score of 3	Score of 2	Score of 1
Type of Collision	In-Line Head-On	In-Line Rear-End	All Other Types
Closing Speed at Impact	Above 70 mph	50 to 70 mph	Below 50 mph
Resulting Casualties	Fatality/Fatal Injury	Severe Injury	Minor Injury

The weighting factor was combined with the ranking metric and assigned the following values:

- For those accidents involving a modern lead locomotive, the weighting factor = 2.
- For all accidents involving a non-modern lead locomotive, the weighting factor = 1.

Using this computational process for the gradation of collision severity in a tabular format, a normalized score is determined by using the following relationship:

$$\text{Normalized Score} = \frac{(\text{Total score for each accident case}) \times (\text{The assigned weighting factor})}{(\text{Maximum possible score (which is 18)})}$$

The team applied this ranking metric technique to shortlist the top five severe collision cases (Table 7). Table 8 lists the STEP-1 ranking metric evaluation process involving the accidents from Task 1.

Table 7. Short Listed, Top Five Severe Collision Cases Based on Normalized Score

SL No.	Normalized Score	NTSB - ID	Lead Locomotive	Manufacturer	Model Number	Manufacture Year	Lead Locomotive
1	1.00	RAR-13-02	UP8692	EMD	SD70ACe	2011	Modern
2	0.67	RAR-21-01	BNSF4283	GE	ES44C4	2016	Modern
3	0.50	RAB-19-02	BNSF5162	GE	C44-9W	2004	Not modern
4	0.50	RAR-16-03	UP9707	GE	C44-9W	1994	Not modern
5	0.44	RAR-15-02	BNSF7891	GE	ES44DC	2010	Modern

Table 8. Ranking Metric Evaluation Process Involving The 22 Accident Cases Identified in Task 1

MODERN FREIGHT LOCOMOTIVE COLLISION SEVERITY EVALUATION THROUGH THE USE OF RANKING METRIC AND WEIGHTING FACTOR														
NTSB REPORT#	Closing Speed at impact (MPH)			Collision Type			Casualties			Total Score	Lead Locomotive - Modern?	Weighting Factor	Normalized Score	Remarks
NTSB ID:	< 50 1	50 - 70 2	> 70 3	Inline/ Head-On 3	Inline/ Rear-end 2	All other types 1	Fatality 3	Fatal/Serious injury 2	Minor/ No injury 1	Sum of all 3 scores	Y / N	X 2 / X 1	Total Score / Max. Possible score(18)	
RAR-21-01	1				2		3			6	Y	X 2	0.67	A modern locomotive was in the lead of a train consist
RAR-20-05		2			2		3			7	N	X 1	0.39	
RAR-20-03	1					1		1		3	N	X 1	0.17	
RAR-19-02		2			3		3			8	N	X 1	0.44	No modern locomotive was in the lead
RAB-1902			3	3			3			9	N	X 1	0.50	A modern locomotive was in the 2nd position of train consist
RAB-1710	1			3				1		5	N	X 1	0.28	
RAB-1708	1					1		1		3	Y	X 2	0.33	
RAB-1701	1					1		1		3	N	X 1	0.17	
RAR-16-03			3	3			3			9	N	X 1	0.5	No modern locomotive was in the lead
RAB-15-08	1					1		2		4	N	X 1	0.22	
RAR-15-02	1				2			1		4	Y	X 2	0.44	A modern locomotive was in the lead of a train consist
RAB-15-04	1					1		1		3	N	X 1	0.17	
RAB-14-14	1			3				1		5	N	X 1	0.28	
RAR-14-02	1					1		2		4	N	X 1	0.22	
RAB-14-05	1					1		2		4	N	X 1	0.22	
RAB-13-03	1				2			2		5	N	X 1	0.28	
RAR-13-02			3	3			3			9	Y	X 2	1.00	The struck train consist had a modern locomotive in the lead
RAR-13-01		2		3				2		7	N	X 1	0.39	
RAB-13-01	1				2			2		5	N	X 1	0.28	
RAR-12-02	1				2		3			6	N	X 1	0.33	
RAB-12-02	1					1		1		3	Y	X 2	0.33	
RAR-10-01			3	3				1		7	N	X 1	0.39	

3.1.2 Step 2: Use of Critical Train Collision Parameters to Evolve Collision Evaluation Criteria

The research team examined the NTSB investigation reports for each severe collision case (including the docket documents, for each of the short listed severe collision cases presented in Table 7) to identify the important pre- and post-collision data that constitute essential input parameters for the FE simulations and crash analysis. All modern freight locomotives comply with 49 CFR Part 229 Appendix E and AAR S-580 crashworthiness requirements to enhance cab crew safety in a collision during routine revenue service operations. However, post-2009 freight train accident investigation data reveal several collision cases involving crew in-cab casualties. The team considered these cases while developing the collision evaluation criteria, aiming to identify severe past collision(s) to use in FEA simulations to determine whether the existing S-580 crashworthiness requirements need further revision.

Modern locomotive collision cases fulfilling all requirements in the parameters of the collision evaluation criteria are rare. Therefore, the team selected the modern locomotive collision cases which included the maximum number of the following parameters:

- The collision case must have at least one colliding modern lead locomotive.
 - This is necessary because the main goal of this project is to assess the crashworthiness performance of modern locomotives.
- The NTSB accident investigation report and the docket documents must be officially released and available for public access.
 - The official release of this information is important, because it contains collision-related data essential for building the finite element (FE) models and conducting the simulation studies.
- The collision should preferably have a high normalized score, including a high score for the type of collision, a higher closing speed at the point of impact, and resultant crew casualty.
- The FE model of the colliding modern locomotive under consideration should be available for collision simulation studies and crashworthiness analyses.
 - The Finite Element Models (FEM) of all available modern road locomotives in operational services are not available and there is no scope, under the present program, to build a new FEM starting from scratch. It is therefore important to have the FEM of the concerned modern locomotive readily available for the analysis in the subsequent tasks.
- The event recorder data of the colliding lead locomotive should be retrievable and accessible for use in the reconstruction of the immediate pre-collision dynamic scenario and post-collision FEA studies.
 - The event recorder fitted to each locomotive is intended to record multiple parameters, including the instantaneous speed with a time stamp and the locomotive engineer's input to the control unit (e.g., throttle control position, engagement of emergency braking, etc.) These data are essential for the simulation and reconstruction of collision scenarios during the FEA. In severe post-collision large scale fires, the event recorder data may be lost. In such instances, the NTSB often takes recourse to retrieve the event recorder data of distributive power locomotive positioned in the middle or rear end of the freight consist.
- The lead locomotive post-collision photographs showing structural damages to the locomotive forebody (including the short-hood and intrusion of the cab crew survivability space, if any) should be available for comparison with the results of FEA simulations, to assess their quality and accuracy. This evidence may also be lost in post-collision fires.
- The pre-collision/post-collision positions and injury status of the colliding locomotive cabin crew should be available in the event of at least one cab-crew surviving to narrate the collision event.
 - The primary goal of improving locomotive crashworthiness is enhancing crew safety in the event of a collision. Post-collision crew survival chances may be evaluated through the reconstruction of a severe collision scenario in which the crew is replaced by Anthropomorphic Test Devices (ATDs), if the above information is preserved.
- The crashworthiness Group Chairman's factual report of investigation should be included in the NTSB docket documents, if applicable.
 - Generally, in the event of a severe railroad accident, the NTSB seeks to evaluate crashworthiness of the involved locomotives through a more thorough

investigation made by a specially appointed crashworthiness group, headed by a chairman.

- The submitted final report is placed in the docket, including the results of its analysis and useful exhibits containing features such as the quiet cabin of EMD SD-70 AC, which has improved crashworthiness features over the old conventional cabins. Photographs of locomotive/cabin structural damages and/or inadequacy of crashworthiness may also be included among the exhibits.
- The chairman of this group is empowered to seek further relevant details (e.g., design, manufacturing, modification) from the locomotive manufacturer to complete the crashworthiness assessment and submit their factual report to the NTSB.

3.2 Task 2 Conclusions

In summary, the research team studied the available NTSB investigation reports and docket documents from the short listed severe accident cases, and based on their research, propose the modern locomotive collision evaluation criteria outlined in this section.

4. Task 3 and Task 4





4.1 Methodology









For Task 3, the research team reviewed the available FE models of modern locomotives and executed an upgrade plan. During Task 4, the team aimed to identify and validate the FE models. The following sections outline key steps to achieving these goals, including the review of FE models, crash test analysis, a visit to the train yard, online research, verification and upgrading of the FE models, and challenges faced during these steps.

4.1.1 Review Crash Test Data

Multiple full-scale dynamic crash tests were conducted at TTC using historical accident data from U.S. railroads. These tests were designed to evaluate the crashworthiness of locomotives and involved various critical scenarios such as in-line collisions, offset collisions, and collisions with road vehicles simulating grade-crossing accidents. The tests provided valuable insights into the behavior of locomotive structures and crew during impacts. Members of the team actively participated in these tests, conducting pre- and post-test data analyses, performing FE analyses, and contributing to the final technical reports. A summary of these tests is presented in [Table 9](#).

Table 9. Available TTC Crash Tests

Test	Test Setup	Post Test
1- Head-on Crash with a Stationary Hopper Car		
2- Grade Crossing Crash with a Log Truck		

<p>3- Grade Crossing Crash with a Steel Coil Truck</p>		
<p>4- Offset Frontal Crash with Covered Hopper Car</p>		
<p>5- Head-on Crash with a Stationary Unloaded Flat Car</p>		
<p>6 & 9- Offset Frontal Crash with Intermodal Container</p>		

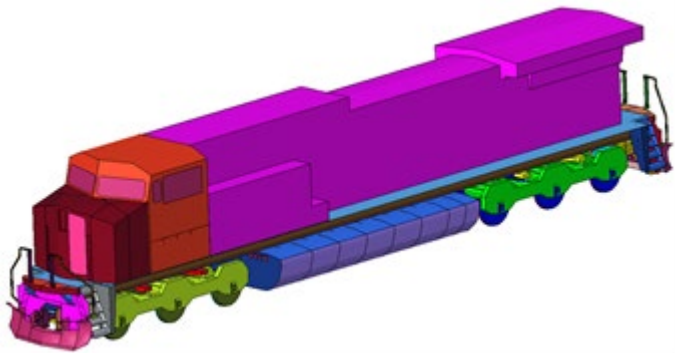
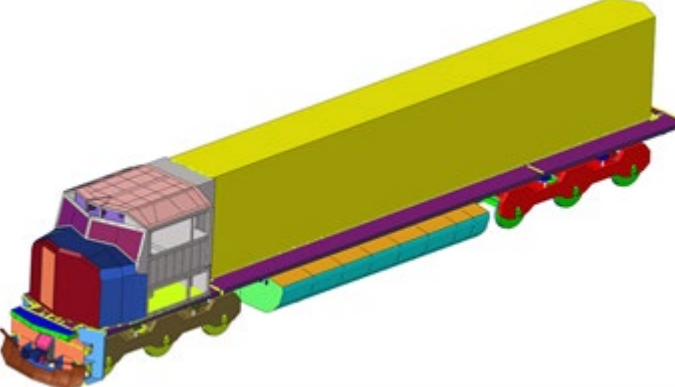
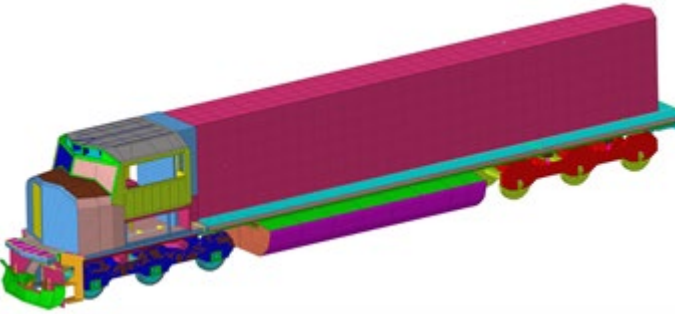

<p>7- Head-on Crash with a Stationary Loaded Hopper Car</p>		
<p>8 & 10- Head-on Crash with a Stationary Loaded Hopper Car - Crew Injury Mitigation</p>		


TTC Test 1, titled (*Full-Scale Locomotive Dynamic Crash Testing and Correlations: Locomotive Consist Colliding with Stationary Hopper Car Consist*), provides valuable insights into locomotive crash dynamics and train car crush, making it a suitable basis for validating FE models. The research team contributed to this test and subsequently conducted an innovative analysis on shock energy absorbers using the same crash scenario. Both the test report and a conference paper based on the test were instrumental in gathering sufficient information to complete Task 4. Test 1 also includes a side view video that proved highly useful during the validation phase, and the report contains initial acceleration data (200 ms). The team made efforts to acquire additional crash test data from FRA and TTC, but no further information was found for any of the tests or models. Considering these factors, the team is confident that Test 1 presents the highest potential for FE validation in Task 4.

4.1.2 Review FEA Models

Members of this research team were actively involved in the development of existing freight locomotive FE models and train cars. In this task, they conducted a comprehensive review and assessment of the current models and identified key FE models that would benefit from an upgrade plan by enhancing fidelity and improving simulation outcomes. The FE models are listed in [Table 10](#).

Table 10. Available FE Models

FE Models	Number of Elements	Number of Parts	Image of the FE Model
AC4400_Loco.k	69333	133	 <p>A 3D finite element model of an AC4400 locomotive. The model is composed of various colored parts: a red and orange cab, a large purple body, blue wheels, and green bogies. The locomotive is shown from a side-on perspective, facing left.</p>
SD70MAC_Loco.k	68517	84	 <p>A 3D finite element model of an SD70MAC locomotive. The model features a red and blue cab, a large yellow body, and red wheels. The locomotive is shown from a side-on perspective, facing left.</p>
SD70MAC-final3.k	123966	99	 <p>A 3D finite element model of an SD70MAC locomotive. The model features a blue and green cab, a large purple body, and red wheels. The locomotive is shown from a side-on perspective, facing left.</p>
Run_Chatsworth_Analysis_1015.k	335070	401	 <p>Two views of a curved finite element model. The top view shows a smooth, curved line composed of many small segments, colored in a gradient from purple to yellow. The bottom view shows a more detailed, segmented representation of the same curve, with individual parts colored in purple, blue, and yellow.</p>

TTC Test 1: Run_32mph_1102.k	369013	527	
---------------------------------	--------	-----	--

While all the models provide a reasonable starting point for conducting Tasks 3 and 4, the FE model used to simulate Test 1 is the most detailed one, and features a detailed mesh for the SD70MAC locomotive and the stationary open-top hopper car. As a result, this model was selected to perform Tasks 3 and 4.

4.1.3 FEA Challenges

In the more than 15 years since the FE models were developed, there have been significant improvements to the LS-DYNA software. The researchers recommended exploring any available CAD data or drawings that were used during the initial model development to execute a major model upgrade. The team devoted considerable time and effort to locate all the original documentation that was utilized in the model development process. However, they encountered difficulties in finding additional information beyond the existing reports and public papers. Given that many years have passed and the data has changed hands among different companies, this proved to be a challenge. To address these limitations, it became necessary to gather additional information. The researchers requested to visit a train yard in order to gain firsthand experience with similar train cars and locomotives.

4.1.4 Train Yard Visit (Mass-Coastal)

The team contacted multiple companies in search of a similar open-top hopper car to the one used in TTC Test 1. [Mass Coastal, Inc.](#) located a comparable closed hopper car, which shares similar functionality with the target open-top hopper car in TTC Test 1. While the closed-top hopper car serves the purpose of transporting grains and materials that require more environmental protection, the car used in the test was an open-top hopper car specifically designed for transporting coal and other earth materials without such concerns. Mass Coastal also offered their assistance to the team for the project. The researchers visited the train yard in Taunton, MA to gather information on train car construction, take overall measurements, identify sheet metal thickness, and scan the back of the hopper car.

Figure 4 and Figure 5 illustrate the closed-top hopper car and locomotive provided by Mass Coastal.

In examining the closed-top hopper car, the researchers observed that the structure of each train car may vary depending on factors such as the manufacturer, year of construction, intended cargo, safety regulations, and available materials. The visit to the train yard greatly expanded the researchers' understanding of train cars, locomotives, and trucks. For example, they gained knowledge about how the truck operates and interacts with the freight wagon. Figure 6 and Figure 7 illustrate a general sketch of a truck and the point of contact between the train car and the truck. The train car is supported by two bogeys on each side of the trucks, allowing it to rotate and rock. Additionally, the train car features a circular recess and a sturdy pin that serves as a pivot point, with gravity holding everything together.



Figure 4. Closed Hopper Car



Figure 5. Mass-Coastal Locomotive



Figure 6. The Point of Contact between the Train Car and the Truck

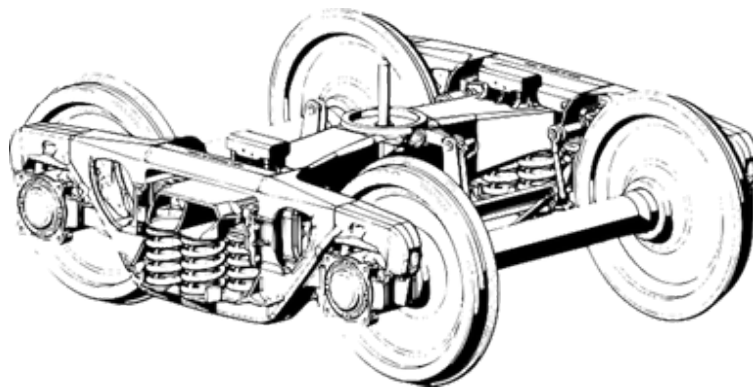


Figure 7. Truck to Train Connections

4.1.5 Review of Available Online Data

The team reviewed online materials for additional information. A [video](#) of a railcar wheel replacement of a train truck by the Thornapple River Rail series was valuable. The video shows how different parts of the trucks are maintained and serviced. The connection to the train car is revealed in [Figure 8](#). This information is helpful for reviewing the truck connections, the stout pin, and their assemblies.



Figure 8. Railcar Wheel Replacement Shows the Stout Pin

4.1.6 FE Model Verifications and Updates

The models have been through many updates and changes. The following sections detail some selected and major changes made to the FE models to prepare them for the validation phase of Task 4.

Units

The units originally used in the FE models were lbf-s²/in, in, and second for the mass, length, and time, respectively. These units were used to calculate force, stress, energy, speed, and acceleration. For comparison, [Table 11](#) displays the corresponding units in the International System of Units (SI), which uses kg, meter, and second for mass, length, and time, respectively. The SI units are widely used in automotive applications. To facilitate their future utilization, all models have been converted to SI.

Table 11. Units and Essential Conversion between SI and Original FE Model Units

MASS	LENGTH	TIME	FORCE	STRESS	ENERGY	Steel DENSITY	Steel YOUNG's	Speed of 35 MPH or 56.33 KPH	GRAVITY
lbf-s ² /in	in	s	Lbf	psi	lbf-in	7.33e-04	3.00e+07	6.16e+02	386
Kg	m	s	N	Pa	N-m = J	7.83e+03	2.07e+11	15.65	9.806

Time Step and Added Mass

The model utilizes a fixed time step of 5 microseconds (μ s). Using a fixed time step introduces additional mass associated with the smallest elements in the models. Simulating a duration of 2 seconds requires approximately 3 hours of computational time using MPP 64 processors on an Intel-MPI 3.2.2 Xeon64 system. To maintain a reasonable computational time, a minimum

element length of 1.0 in (~25 mm) is required for a time step of 5 μ s. The time step plays a crucial role in managing computational time effectively.

Mesh Quality

Figure 9 depicts the original open-top hopper car model, consisting of 42,029 elements (34,820 shell, 7,175 solids, and 34 beam/discrete) and 61 parts. The open-top hopper car is modeled in detail (fine mesh), while all the other train cars are modeled in coarse mesh since they are not directly involved in the crash.

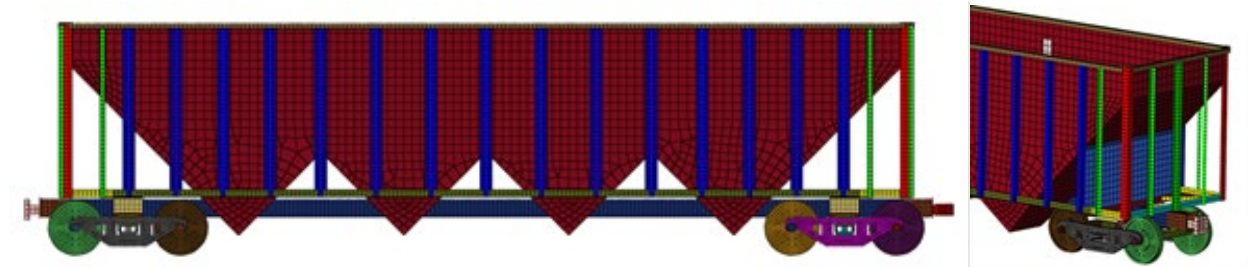


Figure 9. Original Open-Top Hopper Car FE Model

The locomotive of TTC Test 1 crushed only the open-top hopper car. The mesh elements are predominantly coarse, particularly away from the impact zone, and become finer near the location of impact. Employing larger elements would stiffen the model and hinder the reasonable failure of the material or the weld surrounding it. The mesh quality of the model is presented in Table 12.

Table 12. Original Open-Top Hopper Car Model Characteristic

Element Type	Element Criteria	Minimum Value	Number of Elements Failed & their Percentage
Shell	Length < 20 mm	13.5 mm	2648 (7.6%)
	Warpage > 20 deg.	23.7 deg.	8 (0%)
	Jacobian < 0.6	0.35	57 (0.2%)
Solid	Length < 20 mm	8.9 mm	387 (5.4%)
	Warpage > 20 deg.	22.29 deg.	4 (0%)
	Jacobian < 0.6	.52	136 (1.9%)

The open-top hopper car model was revised to accurately reflect the specific car used in TTC Test 1 using images from the report and crash test video. Figure 10 displays the ultimate form of the FE model, while Figures 11 and 12 show the pre-crash images of the open-top hopper car.

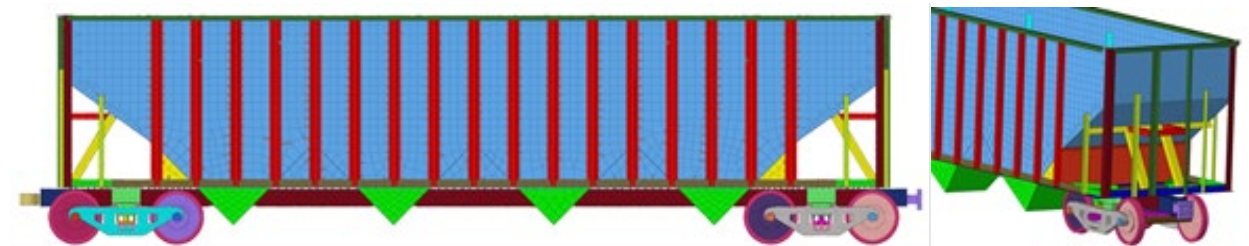


Figure 10. Updated and Modified Open-Top Hopper Car FE Model



Figure 11. Pre-Crash Image of TTC Test 1 Hopper Car



Figure 12. Pre-Crash Image of TTC Test 1 Hopper Car

The model was updated through the implementation of several significant actions:

- Remeshing of the outer shell of the train car
- Remeshing of the rails
- Fixing the characteristics and sizes of the elements
- Modification of the connections between the back and side of the car's outer shell, including the introduction of Spot-welds
- Additional spot-welds to address any apparent missing connections
- Introduction of spot-weld failure

- Introduction of new parts, including:
 - Reinforcement at the back of the car (based on pictures), represented in yellow in the model
 - Vertical reinforcement to match the back of the car, denoted in green in the model.
 - The remodeled back of the car outer shell
- Adjustment of the Smooth Particle Hydrodynamics SPH elements to align with the updated geometric shape.

The total number of elements in the updated model increased to 101,482, comprised of 94,273 shells, 7,175 solids, and 34 beam/discrete elements. Additionally, the revised model consisted of 64 parts. The mesh quality of the model is illustrated in [Table 13](#).

Table 13. Updated Open-Top Hopper Car Model Characteristics

Element Type	Element Criteria	Minimum Value	Number of Elements Failed and their Percentage
Shell	Length < 20 mm	13.5 mm	5332 (5.7-%)
	Warpage > 20 deg.	23.7 deg.	8 (0-%)
	Jacobian < 0.6	0.35	65 (0.1-%)
Solid	Length < 20 mm	8.8 mm	387 (5.4%)
	Warpage > 20 deg.	22.3 deg.	4 (0%)
	Jacobian < 0.6	0.52	136 (1.9%)

Material and Properties

The majority of components in both locomotive and train cars are constructed from steel. The commonly employed material card for steel is *MAT_PIECEWISE_LINEAR_PLASTICITY (Mat_24). Any materials that did not fall under this category were updated to Mat_24. The failure parameters on all material cards were adjusted accordingly.

Connections

In the locomotive model, a single connection was initially used between the cab and the collision posts and the locomotive itself, employing *CONSTRAINED_NODAL_RIGID_BODY. This connection spanned a considerable area, as depicted in the highlighted nodes in [Figure 13](#), and artificially increased the stiffness of the locomotive. To rectify this, the constraint was removed and replaced with multiple spot-welds, enabling local connections among nearby elements.

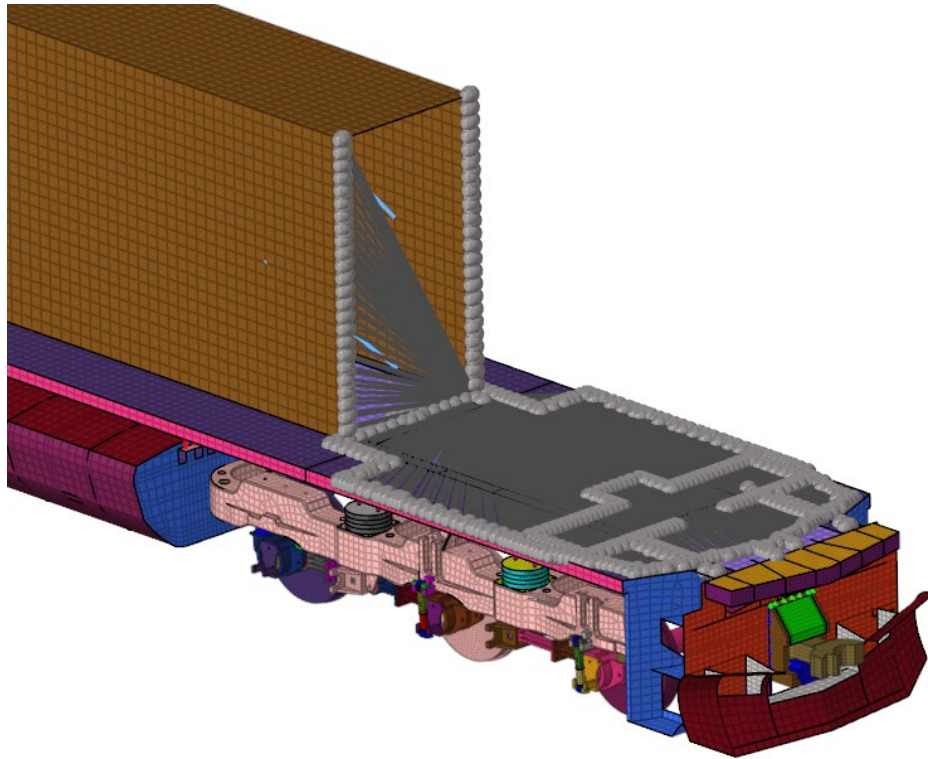


Figure 13. Locomotive Nodal Rigid Body Constraint (Cab and Hood Not Shown)

Spot-Weld

The spot-welds in the open-top hopper car were revised to incorporate failure with the filter option. The `*CONSTRAINED_SPOTWELD` cards were replaced with `*CONSTRAINED_GENERALIZED_WELD_SPOT`. The latter constraint in the LS-DYNA card includes a filter option that allows for the averaging of forces obtained from the model. This enables the application of spot-weld failure when necessary, providing a reliable means to accurately represent the real weld in the train car without any data noise.

Joints

In the original model, the joints at the locomotive wheel sets were not rotating. Instead, they were sliding along the rails and causing deceleration of the locomotive. This issue was due to over-constraining of the joints in the model. The nodes of the `*CONSTRAINED_JOINT` were adjusted to accurately capture the correct behavior of the wheels by revising the component attachments, axes of rotation, and joint types.

4.2 FE Model Validation

This section focuses on the model setup and simulation results. The simulations were conducted using LS-DYNA version based on mpp s R11.1.0.

4.2.1 Model Setup

TTC Test 1 involved a locomotive and three-consist cars colliding with a stationary, 36-consist train at a speed of 32.1 mph. The original test is illustrated in Figure 14.

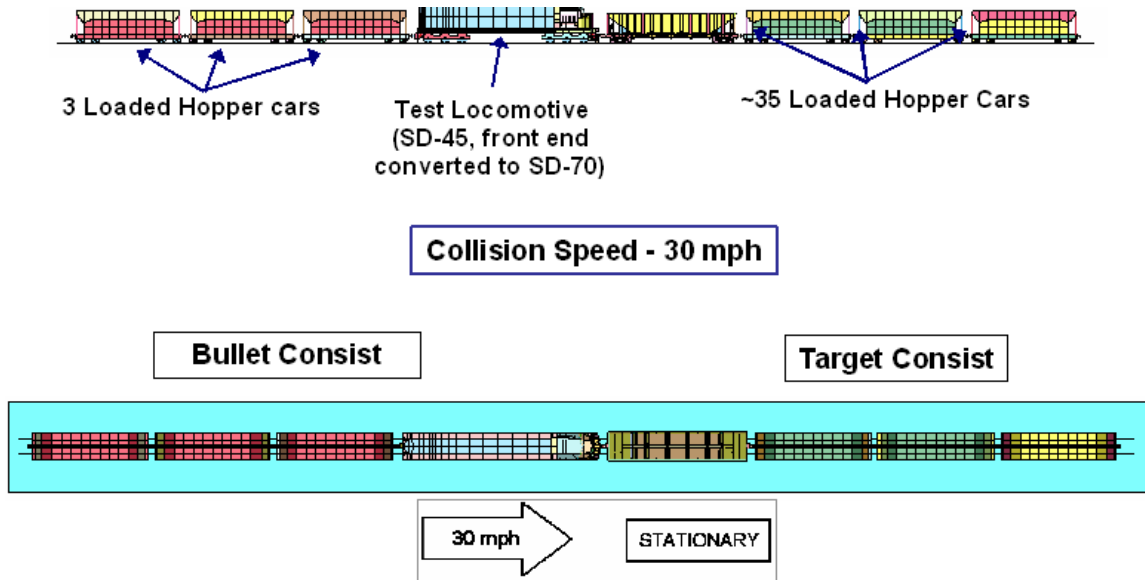


Figure 14. Original Model Setup (From TTC Test 1 Report)

The three bullet consist car models positioned behind the locomotive are depicted in Figure 15. These models utilize a coarse mesh, comprised of 6,250 elements (3,330 shell, 2,914 solids, and 6 beam/discrete) and 17 parts. The mesh predominantly consists of elements larger than 50.8 mm (2 inches), and approximately 10.1 percent of elements are larger than 508 mm (20 inches). The Jacobian and warpage values are negligible. Additionally, the train car section located behind the locomotive is modeled with a finer mesh.



Figure 15. Three Consist Car Models Used Behind the Locomotive

The first target consist car model used is shown in Figure 16. This model utilizes a fine mesh, comprised of 101,482 elements (94,273 shell, 7,175 solids, and 34 beam/discrete) and 64 parts. The mesh predominantly consists of elements larger than 50.8 mm (2 inches), and approximately 6.0 percent of elements are smaller than 25.4 mm (1 inch). The Jacobian and warpage values are negligible. This open-top hopper car weighs about 200,000 lbf (90.7 tons). To match the target consist, the coarse consist shown in Figure 15 was repeated multiple times in lines. The total number of consists behind the stationary open-top hopper car is 35 cars. The stationary freight consist has a weight of 9,100,000 lbf (~4,127.7 tons). The average car weight is approximately 252,000 lbf (114 tons).

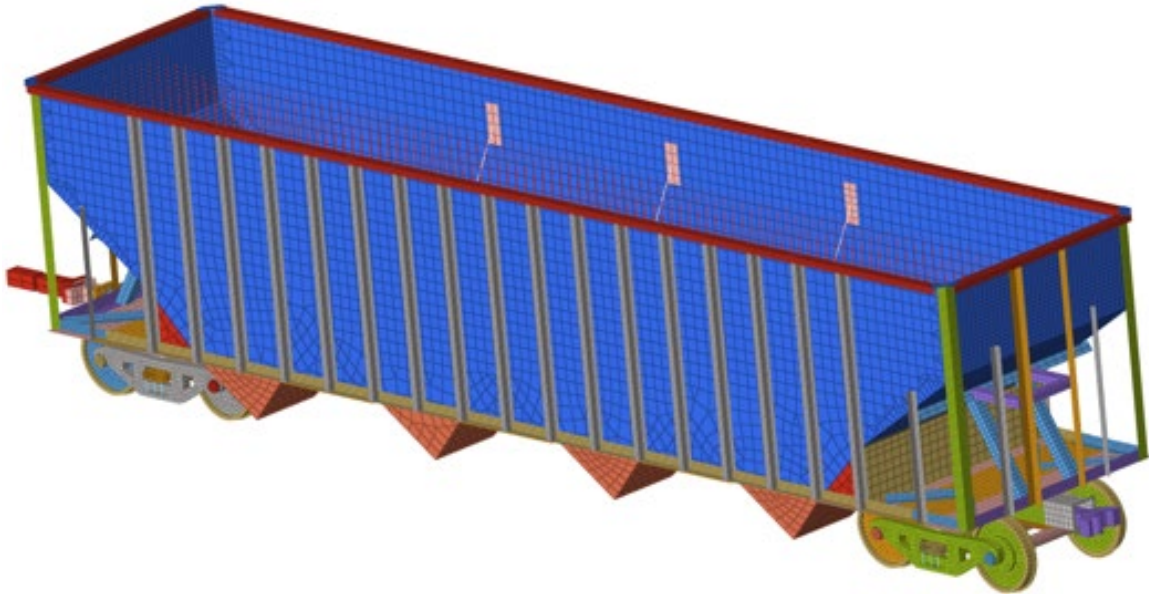


Figure 16. Modified Open-Top Hopper Car FE Model

The locomotive unit and the three freight consist bullet cars have a combined weight of 1,185,900 lbf (537.9 tons), with the locomotive weighing 310,870 lbf (141 tons). The modified test setup is depicted in [Figure 17](#), which depicts a close-up view of the locomotive and the open-top hopper car with fine mesh model, and [Figure 18](#), an illustration of the entire system.



Figure 17. Close-Up of the Updated Model Setup



Figure 18. Overview of the Updated Model Setup

4.2.2 Simulation Comparison

The FE model was used to simulate the model setup described in the previous section and the TTC test. The key findings and results are discussed in the following sections.

Key Validation Comparisons

The sequential side-by-side views in [Figure 19](#) through [Figure 30](#) show the right side view of the locomotive and bullet consist impacting the stationary consist at 32.1 mph. At 250 ms, the locomotive began crushing the open-top hopper car, which started to lift up above the track rails. At 600 ms, the locomotive was lifted above the open-top hopper car rails and began to crush the back of the car outer shell. At 800 ms, the locomotive continued pushing forward and climbing, and tore through the car outer shell. The connections between the corner reinforcement and the

car outer shell began to open, allowing the SPH elements to move out of the way. The locomotive kept moving forward, displacing the coal and pushing the side panels of the open-top hopper car outward. This process continued until the 2-second mark. The locomotive and the open-top hopper car in the crash test exhibited similar behavior to the simulation.

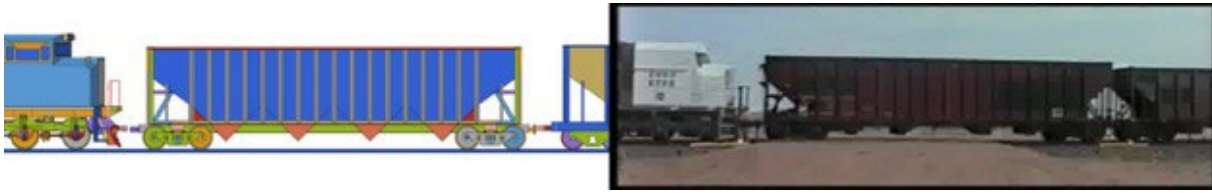


Figure 19. Sequential Images between Simulation and TTC Crash Test at 0 ms

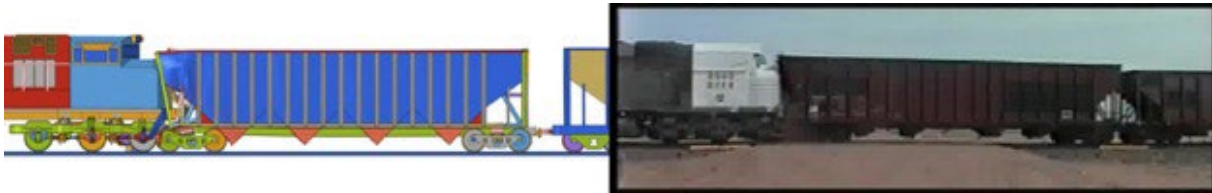


Figure 20. Sequential Images between Simulation and TTC Crash Test at 200 ms



Figure 21. Sequential Images between Simulation and TTC Crash Test at 400 ms

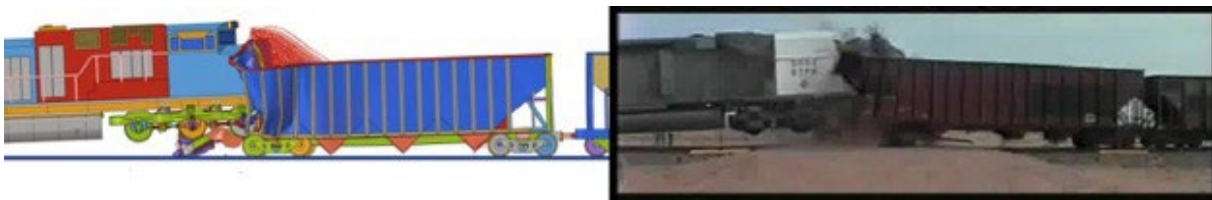


Figure 22. Sequential Images between Simulation and TTC Crash Test at 600 ms



Figure 23. Sequential Images between Simulation and TTC Crash Test at 800 ms

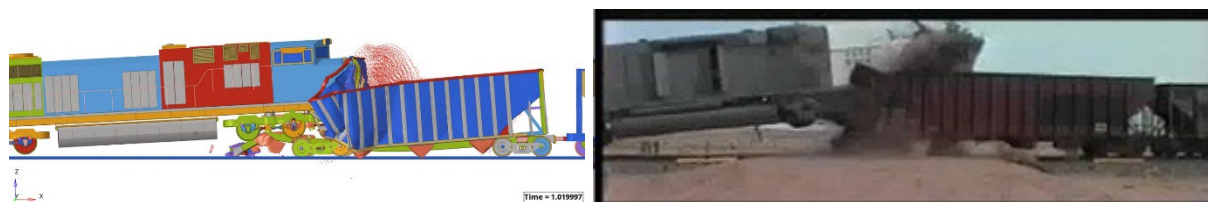


Figure 24. Sequential Images between Simulation and TTC Crash Test at 1,000 ms

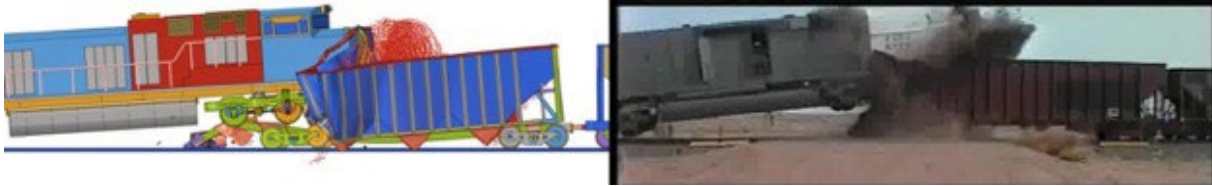


Figure 25. Sequential Images between Simulation and TTC Crash Test at 1,200 ms

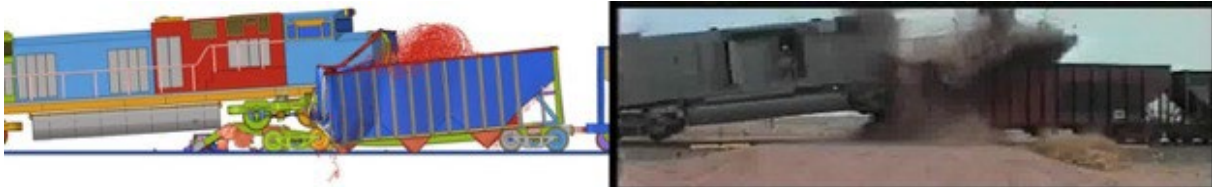


Figure 26. Sequential Images between Simulation and TTC Crash Test at 1,400 ms



Figure 27. Sequential Images between Simulation and TTC Crash Test at 1,600 ms



Figure 28. Sequential Images between Simulation and TTC Crash Test at 1,800 ms



Figure 29. Sequential Images between Simulation and TTC Crash Test at 1,900 ms

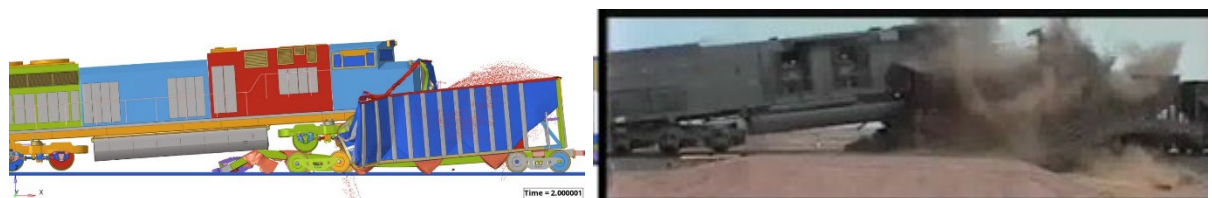


Figure 30. Sequential Images between Simulation and TTC Crash Test at 2,000 ms

Post-impact images comparing the test and simulation are shown in [Figure 31](#) and [Figure 32](#). The image of the test in [Figure 32](#) demonstrates the extent of damage experienced by the hopper car. Viewed from the left-hand side of the locomotive, one sliding gate of the hopper car (i.e., the underneath door for discharging the freight load) has been completely crushed, while the truck of

the hopper car has been pushed forward and stopped just before the second sliding gate (see arrow). This position of the truck was determined by closely examining the original image in Figure 12. The side wall of the hopper car exhibits black paint (see circle) that extends from the beginning of the slope section (near the end of the car) up to the second sliding gate (Figure 12). Figure 32 displays only the end of the black paint near the middle of the hopper car.

Both images of the test in Figure 31 and Figure 32 appear to be taken from the left-hand side of the locomotive. The picture in Figure 31, taken after the crash, shows the extended lateral section of the hopper car's side wall outer shell (see circle). The picture in Figure 32 reveals a missing portion of that side wall outer shell. It appears that the extended lateral section of the side wall was taken away from the hopper car during the removal of the locomotive. The team investigated these images carefully, examined the tearing, fine-tuned the spot-weld failure, and utilized the correct modeling techniques to enhance the validation.

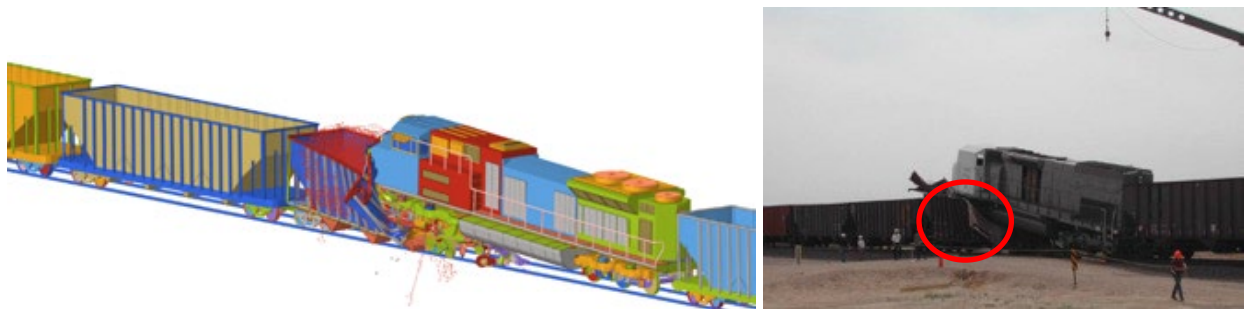


Figure 31. Post-Impact Crush Comparisons, Overview



Figure 32. Post-Impact Crush Comparisons, Close-Up

4.3 Task 3 and Task 4 Conclusions

In summary, the team conducted a thorough review of the available TTC crash tests and FE models. They selected the test that provided the most comprehensive information and used the corresponding FE models for validations. Subsequently, the FE models underwent meticulous upgrades and simulations to accurately replicate the crash test. Through multiple iterations and improvements, the FE model successfully captured the essential aspects of the crash test, indicating its validation.

5. Task 5

5.1 NTSB Cases Summary

The aim of Task 5 was to conduct specific collision simulation of the top selected collision case identified in Task 2. The following sections summarize each case and describe efforts to collect additional evidence, including review of news websites.

5.1.1 Review of Crash RAR-13-02: Head-On Collision of Two Union Pacific Railroad Freight Trains Near Goodwell, Oklahoma; June 24, 2012

NTSB case RAR-13-02 (NTIS report PB2013-107679/DCA12MR005; [Table 14](#)) had a high normalized score according to the ranking metric. The case involved a head-on collision of two Union Pacific Railroad freight trains on June 24, 2012, in Goodwell, Oklahoma. The eastbound train was traveling at 58 mph and the westbound train at 21 mph, with an estimated closing collision speed of 79 mph. The accident occurred on a straight track with a grade of 0.5 percent to the west. The eastbound train was ZLAAH-22 and the westbound train was AAMMLX-22.

Table 14. Train Crash RAR-13-02 Summary

Normalized Score	NTSB ID	Lead Locomotive	Manufacturer	Model Number	Year of Manufacture	Locomotive Types	Docket Link ID
1.00	RAR-13-02	UP8692	EMD	SD70ACe	2011	Lead Modern Locomotive	DCA12MR005

The accident caused severe damage and multiple fatalities. The eastbound locomotive crew lost two members. The westbound train's engineer also perished, and the conductor sustained injuries. The NTIS Report number is PB2013-107679/DCA12MR005. The incident resulted in the derailment of 3 locomotives and 24 cars of the eastbound train and 2 locomotives and 8 cars of the westbound train, causing the release of fuel and a large fire. The eastbound locomotives involved in the accident were UP8542 (lead), UP5482 (second), and UP7914 (third), built between 2005 and 2008. The westbound locomotives were UP8692 (lead) and UP4855 (second), built in 2011. All locomotives were retired due to the extensive damage caused by the fire, estimated to be approximately \$14.8 million. Three post-crash pictures are presented in the following two pages.



Figure 33. NTSB RAR-13-02 Head-On Collision Near Goodwell, OK, Overview



Figure 34. NTSB RAR-13-02, Close-Up



Figure 35. NTSB RAR-13-02, Wreckage Close-Up

5.1.2 Review of Crash RAR-21-01: BNSF Railroad Collision, Kingman, Arizona; June 5, 2018

Based on its higher normalized score, NTSB case RAR-21-01 (NTIS Report RRD18FR009; [Table 15](#)) ranked second of the cases in [Table 7](#), Task 2. The case involved a collision on June 5, 2018, in Kingman, Arizona. The collision involved a westbound BNSF Railway Intermodal train (designated S MEMSCO1 02L) colliding with the rear of an eastbound rail-laying work train (designated WNEESGM1 05). At the time of the collision, the westbound train was traveling at 15 mph on multiple main tracks and the eastbound train was traveling at a slower speed of 9 mph. The railroad track at the accident site had an 8-degree sharp curve and a downgrade of 1.5 percent grade to the east.

The collision caused two fatalities and resulted in severe damage to the rail unloading machine (RUM) that was attached to the rear of the eastbound train. The westbound intermodal locomotive train also derailed. The eastbound work train had 2 forward-facing locomotives and 29 cars, including the RUM, while the westbound intermodal train had one forward-facing and two rear-facing locomotives and 72 loaded cars. The eastbound train was 1,900 feet long and weighed 3,830 tons, while the westbound train was 6,574 feet long and weighed 8,186 tons. The lead locomotive for the westbound train was BNSF4283, built in 2016. Three post-crash pictures are presented in the following two pages.

Table 15. Train Crash RAR-21-01 Summary

Normalized Score	NTSB ID	Lead Locomotive	Manufacturer	Model Number	Year of Manufacture	Locomotive Types	Docket Link ID
0.67	RAR-21-01	BNSF4283	GE	ES44C4	2016	Lead Modern Locomotive	RRD18FR009



Figure 36. NTSB RAR-21-01 BNSF Railroad Collision Near Kingman, AZ, Overview



Figure 37. NTSB RAR-21-01 BNSF Railroad Collision Near Kingman, AZ, Wreckage Close-Up



Figure 38. NTSB RAR-21-01 BNSF Railroad Collision Near Kingman, AZ, RUM from CWR Work Train (Source: BNSF)

5.1.3 Review of Crash RAR-19-02: Amtrak Passenger Train Head-on Collision With Stationary CSX Freight Train, Cayce, South Carolina; February 4, 2018

NTSB RAR case 19-02 (NTIS Report PB2019-101308/DCA16FR008; Table 16) ranked third of the crash cases in Table 7, Task 2. The NTSB report is titled *Amtrak Passenger Train Head-on Collision With Stationary CSX Freight Train, Cayce, South Carolina; 2/4/2018*. The accident occurred in Cayce, South Carolina, on February 4, 2018. The southbound Amtrak passenger train (identified as P91) was traveling at 50 mph when it collided head-on with the northbound stationary CSX freight train (F777), with an estimated accident closing speed of 50 mph.

The collision resulted in severe damage and multiple fatalities, including the death of the southbound locomotive's engineer and conductor. The southbound train had one locomotive, three passenger coaches, one lounge car, two sleeper cars, and a baggage car. The estimated damage was approximately \$25.4 million. The northbound train struck lead locomotive identification number was CSX130, and the second was CSX36. The locomotive identification number for the southbound train was AMTK47.

Table 16. Train Crash RAR-19-02 Summary

Normalized Score	NTSB ID	Lead Locomotive Number	Manufacturer	Model Number	Year of Manufacture	Locomotive Types	Docket Link ID
0.5	RAR-19-02	BNSF5162	GE	C44-9W	2004	Not Modern Locomotive	DCA16FR008



Figure 39. NTSB RAR-19-02, Ariel View

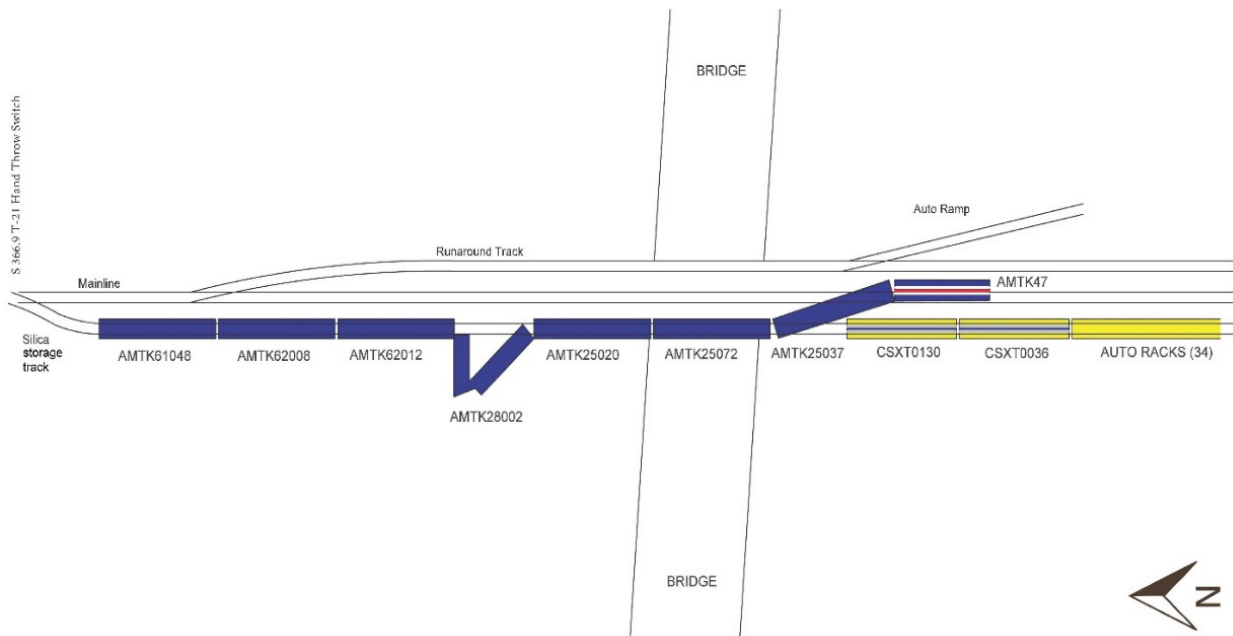


Figure 40. NTSB RAR-19-02, Overview Resting Position



Figure 41. NTSB RAR-19-02, Overview



Figure 42. NTSB RAR-19-02, Front Locomotive

5.1.4 Review Crash RAR-16-03: Collision of Two Union Pacific Railroad Freight Trains, Hoxie, Arkansas; August 17, 2014

NTSB RAR case 16-03 (NTIS Report PB2017-100970/DCA14FR011; [Table 17](#)), titled *Collision of Two Union Pacific Railroad Freight Trains Hoxie, Arkansas on 8/17/2014*, ranked fourth in [Table 7](#), Task 2. At the time of the collision, the southbound train was traveling at 45 mph and the northbound train at 35 mph. The southbound Union Pacific Railroad freight train was identified as IMASNL-16, and the northbound Union Pacific freight train was IQNLPI-17.

The collision caused severe damage and resulted in multiple fatalities. Two crew members from the southbound train died, and the northbound engineer and conductor suffered serious injuries. The southbound train consisted of 2 locomotives and 86 cars, while the northbound train had 2 locomotives and 92 cars. The locomotives from both trains derailed, and the second locomotive from the northbound train released diesel fuel, resulting in a fire. A total of 55 cars derailed: 41 from the southbound train and 14 from the northbound train. The estimated damage was about \$10.7 million.

The southbound train had a total length of 5,468 feet and weighed 7,241 gross tons, with 47 loaded and 39 empty cars. The northbound train was 5,896 feet long and weighed 9,478 gross tons, with 71 loaded and 21 empty cars. The leading locomotive identification number for the southbound train was UP9707, while the northbound train was led by UP5070, with UP4530 as its second locomotive.

Table 17. Train Crash RAR-16-03 Summary

Normalized Score	NTSB ID	Lead Locomotive Number	Manufacturer	Model Number	Year of Manufacture	Locomotive Types	Docket Link ID
0.5	RAR-16-03	UP9707	GE	C44-9W	1994	Not Modern	DCA14FR011



Figure 43. NTSB RAR-16-03, Overview



Figure 44. NTSB RAR-16-03, Southbound Locomotive

5.1.5 Review Crash RAR-15-02: Collision Involving Three BNSF Railway Freight Trains near Amarillo, Texas, September 25, 2013

NTSB RAR case 15-02 (NTIS Report PB2015/105169/DCA13FR013; [Table 18](#)) ranked fifth in [Table 7](#), Task 2. The NTSB report, titled *Collision Involving Three BNSF Railway Freight Trains near Amarillo, Texas, 9/25/2013*, involved a collision between three BNSF freight trains. The eastbound train collided with the rear end of a stationary BNSF train on track 2, causing derailment of some cars onto track 1, which were then hit by an approaching westbound BNSF train. The eastbound train was traveling at 26 mph and was identified as BLACWSP223A while the stationary train was SLHTLPC223A. Five out of six train crewmembers were injured and hospitalized. The estimated damage from the incident was around \$4.4 million.

Table 18. Train Crash RAR-15-02 Summary

Normalized Score	NTSB ID	Lead Locomotive Number	Manufacturer	Model Number	Manufacture Year	Locomotive Types	Docket Link ID
0.44	RAR-15-02	BNSF7891	GE	ES44DC	2010	Lead Modern Locomotive	DCA13FR013 (Not yet publicly released)

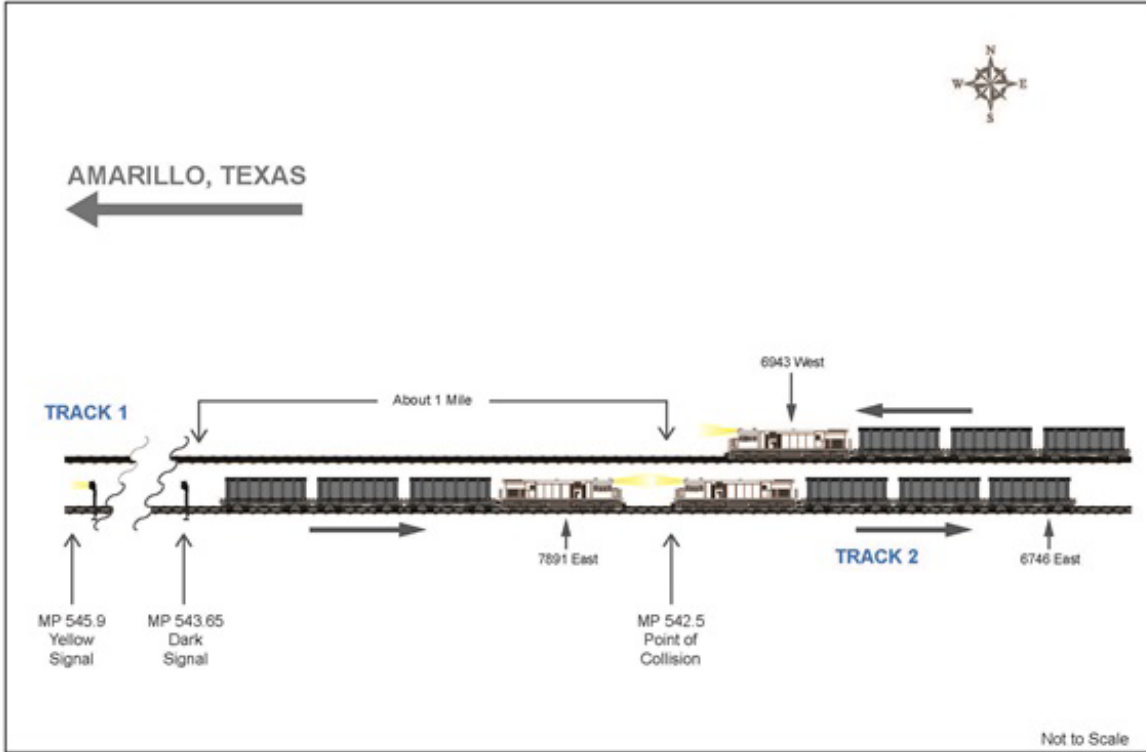


Figure 45. NTSB RAR-15-02, Overview Resting Position



Figure 46. NTSB RAR-15-02, Overview



Figure 47. NTSB RAR-15-02, Close-up View

5.2 Updated and New FE Models

Since the submission of Tasks 3 and 4, the locomotive FE model has undergone significant updates and changes. These modifications have led to better validation of Task 4. To simulate NTSB crash case RAR 13-02, additional FE models were created from the existing train cars. Details about the NTSB crash simulation are discussed in the following section. All simulations were performed using LS-DYNA version "mpps R11.2.2" released on May 3, 2021.

5.2.1 Units

The FE models were originally created using the system of units lbf-s²/in, inch, and second for mass, length, and time, respectively. However, the research team decided to switch to the International System of Units (SI), widely used in the automotive crashworthiness field, for mass, length, and time. [Table 19](#) shows a comparison of the units used for force, stress, energy, speed, and acceleration, and the corresponding calculations for each unit are provided.

Table 19. Units and Conversion Equations between SI and Original FE Model Units

MASS	LENGTH	TIME	FORCE	STRESS	ENERGY	Steel DENSITY	Steel YOUNG'S	Speed of 35 MPH or 56.33 KPH	GRAVITY
lbf-s ² /in	in	s	Lbf	psi	lbf-in	7.33e-04	3.00e+07	6.16e+02	386
Kg	m	s	N	Pa	N-m = J	7.83e+03	2.07e+11	15.65	9.806

5.2.2 Time Step and Added Mass

Previously, the FE model employed a fixed time step of 4 μ s to ensure computational efficiency, but this led to an increase in mass (added mass) associated with the smallest elements of the models. As a result, the locomotive wheels experienced an additional mass, which impacted the validation of the FE model in Task 4. To address this issue, the research team modified the time step to 0.5 μ s, resulting in longer computation time but more accurate validation.

5.2.3 FE Models Review

The FE models were modified, and new train cars were added to generate additional models needed for the NTSB crash case. Significant changes were made to the locomotive's body, and its structure was revised to accurately represent its behavior. Two main types of consists were developed to capture the freight car characteristics, based on the original train car models.

Updated Locomotive Model

The SD70MAC locomotive was updated to capture the main functional features of the locomotives. The cab, frame, fuel tanks, and trucks were maintained, but the structure behind the cab was remodeled to capture the engine compartment, cooling compartment, air compressor system, etc. The model connections were revised and improved, and the joints were adjusted to capture the correct wheel behavior. The latest FE model is version 5, while the original model was version 2. [Figure 48](#) and [Figure 49](#) show a comparison between FE model version 5 and a generic locomotive. The total number of parts, elements, and rigid elements between both FE models are compared in [Table 20](#).

Table 20. Original and Updated FE Models Details of the SD70MAC Locomotives Comparisons

Locomotive	Total Number of Elements	Total Number of Parts	Solid Elements	Shell Elements	Beam Elements	Rigid Elements	Nodal Rigid Elements
Ver 02 (Orig)	316,471	369	218,107	98,107	171	80,512	639
Ver 05	351,102	372	218,533	130,535	2,014	161,850	663

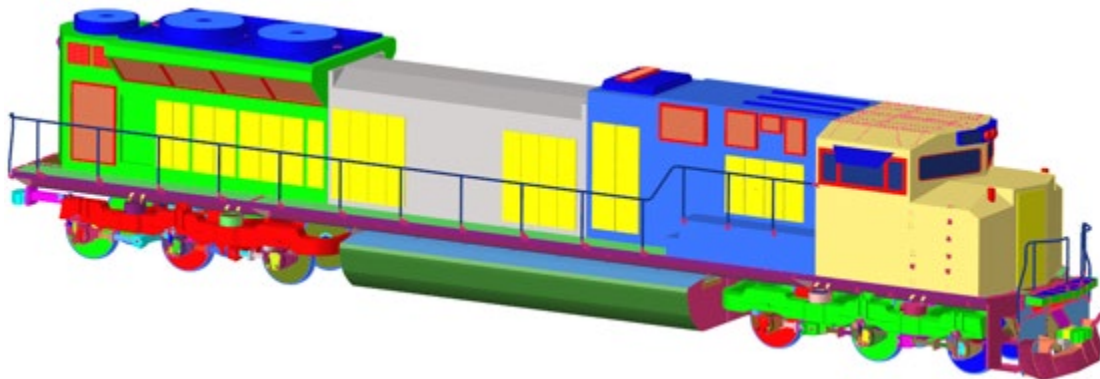


Figure 48. SD70MAC Locomotive FE Model



Figure 49. Actual Locomotive for Comparison (Wikimedia Commons)

New Ship Car Model

To simulate the NTSB case, the team needed to create consists for the freight train. The ship cars are used to move shipping (intermodal) containers on either well cars or flat cars. For the case of interest, the flat cars ([Figure 50](#)) were used since the FE model was available. The train cars were only derailed in the crash and were not directly involved in the crash impact zone. The new ship consists were based on the original train car models and the container models were added to them. [Figures 50](#) and [51](#) show a comparison between FE model and a generic ship car. The total numbers of parts, elements, and rigid elements of the FE model are shown in [Table 21](#).



Figure 50. NTSB RAR-21-01 BNSF Railroad Collision Near Kingman, AZ, Overview (Source: Oklahoman.com)

Table 21. FE Model Details of the Ship Consist Car

Locomotive	Total Number of elements	Total Number of Parts	Solid Elements	Shell Elements	Beam Elements	Rigid Elements	Nodal Rigid Elements
Ship Consist Car	12,252	20	2,612	9,634	0	3,302	0

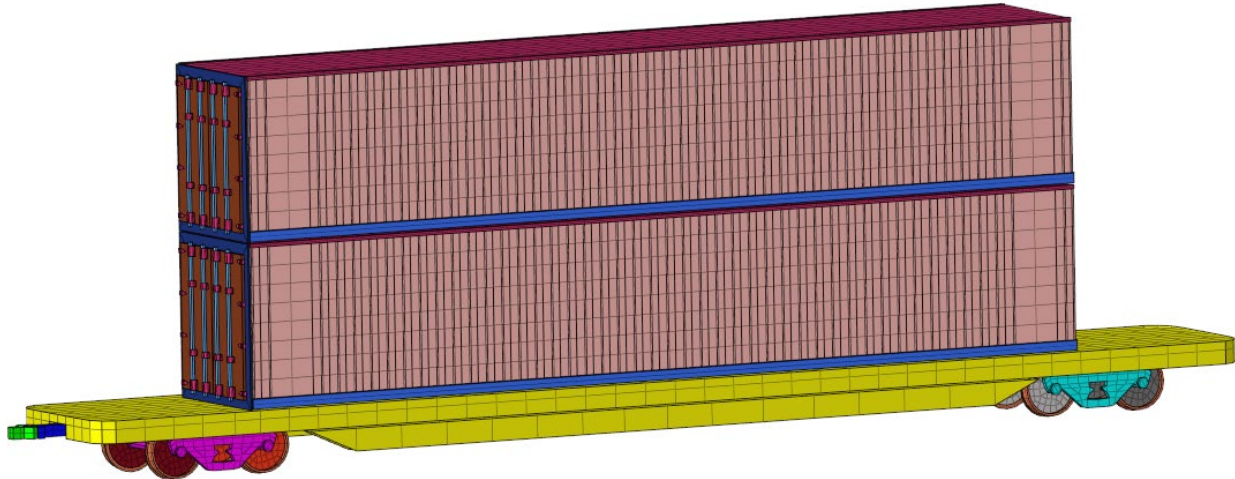


Figure 51. Ship Car FE Model



Figure 52. Actual Ship Car for Comparison, Overview (Source: Wikipedia)

New Auto-Rack Car Model

Similar to the ship car, an auto-rack car also needed to be created (Figure 53). The new auto-rack car was based on the original train car models and the outside structures were added to it. The total number of parts, elements, and rigid elements is shown in Table 22.

Table 22. FE Model Details of the Auto-Rack Car

Locomotive	Total Number of elements	Total Number of Parts	Solid Elements	Shell Elements	Beam Elements	Rigid Elements	Nodal Rigid Elements
Ship Consist Car	22,446	19	2,862	19,578	0	4,814	0

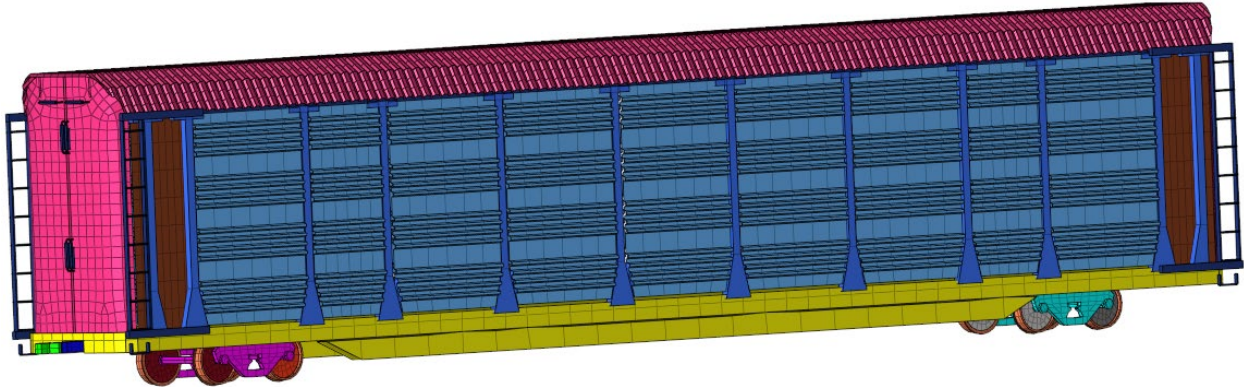


Figure 53. FE Model of the Auto-Rack Car



Figure 54. Actual Auto-Rack Car for Comparison (Source: Wordpress/lionel-llc)

5.3 NTSB Crash Case RAR 13-02 Simulation

NTSB Crash Case RAR 13-02 ranked the highest in [Table 7](#), Task 2. The following sections review the model setup, the simulation results, and how they compare to the actual crash.

5.3.1 Model Setup Summary

The eastbound UPRC freight train (ZLAAH22) included four diesel-electric locomotives: three at the head-end and one at the aft-end of the train. The train had 108 freight railroad cars loaded with double-stacked ISO-type intermodal shipping containers. The train weighed approximately 6,328 tons (gross), and had an overall length of 7,915 ft, including locomotives. A close-up view of the first three locomotives and one ship container car is shown in [Figure 55](#), while [Figure 56](#)

provides an accurate representation of the entire train, consisting of the four locomotives and the 108 ship container cars.



Figure 55. NTSB RAR 13-02 Eastbound UPRC Freight Train, Close-up



Figure 56. NTSB RAR 13-02 Eastbound UPRC Freight Train, Overview

The westbound UPRC freight train (AAMMLX22) was powered by three diesel-electric locomotives: two at the head-end and one at the aft-end of the train. The train consisted of 80 freight cars, all of which were multilevel loaded with motor vehicles, including sedans, vans, and pickup trucks. The train weighed approximately 5,760 tons (gross), and was approximately 7,743 feet overall. [Figure 57](#) shows a close-up view of the first two locomotives and one auto-rack car. [Figure 58](#) depicts the entire train, consisting of the three locomotives and the 80 auto-rack cars, and does not display any details of the model, but provides an accurate representation of the train.



Figure 57. NTSB RAR 13-02 Westbound UPRC Freight Train, Close-up



Figure 58. NTSB RAR 13-02 Westbound UPRC Freight Train, Overview

[Figure 59](#) depicts a detailed view of the collision site, capturing the front three locomotives and two shipping container cars of the eastbound train, as well as the first two locomotives and two auto-rack cars of the westbound train. [Figure 60](#) and [Figure 61](#) provide an overview of the

collision scene, encompassing both trains. The total length of the trains combined is approximately 15,658 ft, or 3 miles. The eastbound train was moving at 58 mph, while the westbound train was traveling at 21 mph. The initial velocity was assigned to the FE models from their respective perspectives.



Figure 59. NTSB RAR 13-02 Eastbound and Westbound UPRC Freight Trains at Impact, Close-up

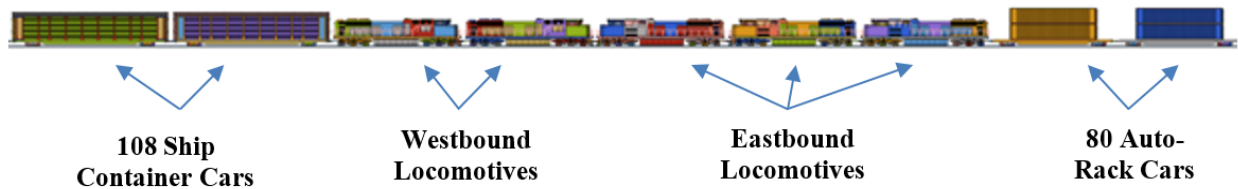


Figure 60. NTSB RAR 13-02 Eastbound and Westbound UPRC Freight Trains at Impact, Overview



Figure 61. NTSB RAR 13-02 Eastbound and Westbound UPRC Freight Trains at Impact, Overview

Table 23 presents the total count of components, elements (by types), and rigid elements utilized in constructing the FE models for both trains. The eastbound locomotive units and freight cars had a combined weight of 6,328 tons, whereas the westbound locomotive units and freight cars weighed 5,760 tons.

Table 23. FE Model Details of Both Trains

Locomotive	Total Number of elements	Total Number of Parts	Solid Elements	Shell Elements	Beam Elements	Rigid Elements	Nodal Rigid Elements
Ship Consist Car	778,463	955	232,138	545,667	521	450,550	865

5.3.2 Simulation Results

Using LS-DYNA software, the model setup outlined in the previous section was simulated for 20 seconds, using 128 processors. The wall time of the simulation took 33 hours. At the end of the simulation time, the trains still had kinetic energies and the simulation still needed additional calculation time.

As a result of the collision, the 3 head-end locomotives and the first 24 platforms (freight cars) of the eastbound train derailed, while the westbound train experienced derailment of its 2 head-end locomotives and 8 freight cars. The locomotives released fuel, which caused a significant fire that lasted over 24 hours. The leading locomotives were all decommissioned, and no detailed

pictures were available of the locomotives following the fire's extinguishment. The subsequent sections discuss the visual findings and simulation stability.

Visual Comparisons

Figure 62 through Figure 77 present a sequential of top-view illustrations from the simulation spanning up to 15 seconds, depicting the derailment of all front locomotives and freight cars. The figures provide insight into how the derailment occurred. The simulation of the eastbound train exhibits 22 derailed cars, whereas the westbound train shows 12 derailed cars. The derailed cars are not precisely aligned with the actual crash; this deviation may be due to the absence of terrain soil modeling surrounding the track, the slope on either side of the track, other related data that may be missing, or additional simulating time.



Figure 62. FE Simulation Results, 0 second

1: LS-DYNA user input
Loadcase 1 : Time = 0.999998 : Frame 6



Figure 63. FE Simulation Results, 1 second

1: LS-DYNA user input
Loadcase 1 : Time = 1.999996 : Frame 11



Figure 64. FE Simulation Results, 2 seconds

1: LS-DYNA user input
Loadcase 1 : Time = 2.999994 : Frame 16



Figure 65. FE Simulation Results, 3 seconds

1: LS-DYNA user input
Loadcase 1 : Time = 3.999997 : Frame 21



Figure 66. FE Simulation Results, 4 seconds

1: LS-DYNA user input
Loadcase 1 : Time = 4.999995 : Frame 26



Figure 67. FE Simulation Results, 5 seconds

1: LS-DYNA user input
Loadcase 1 : Time = 5.999992 : Frame 31

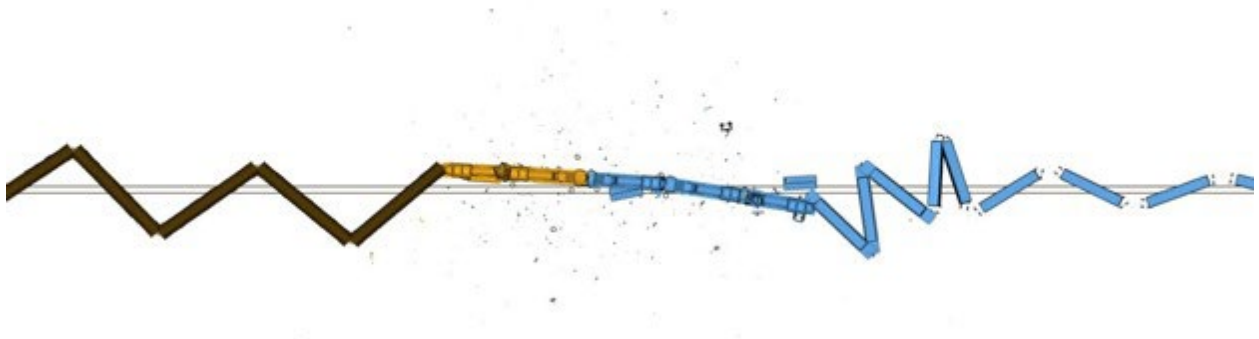


Figure 68. FE Simulation Results, 6 seconds

1: LS-DYNA user input
Loadcase 1 : Time = 6.999990 : Frame 35

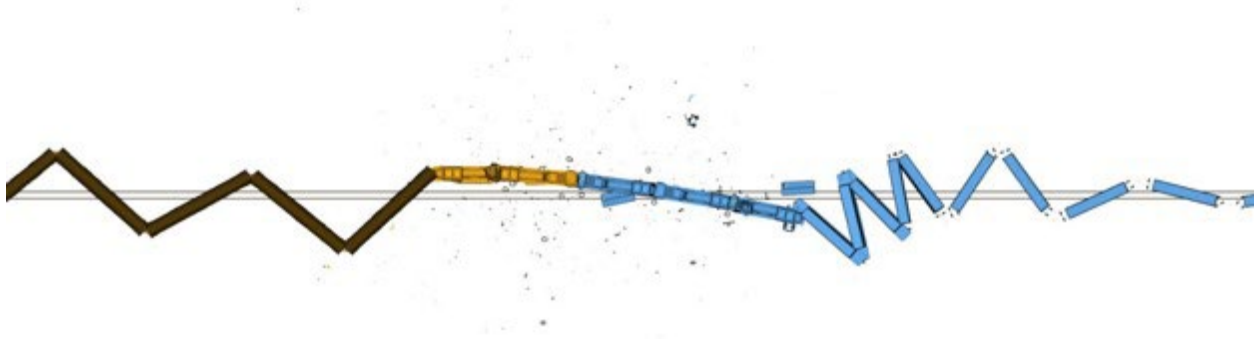


Figure 69. FE Simulation Results, 7 seconds

1: LS-DYNA user input
Loadcase 1 : Time = 7.999989 : Frame 40

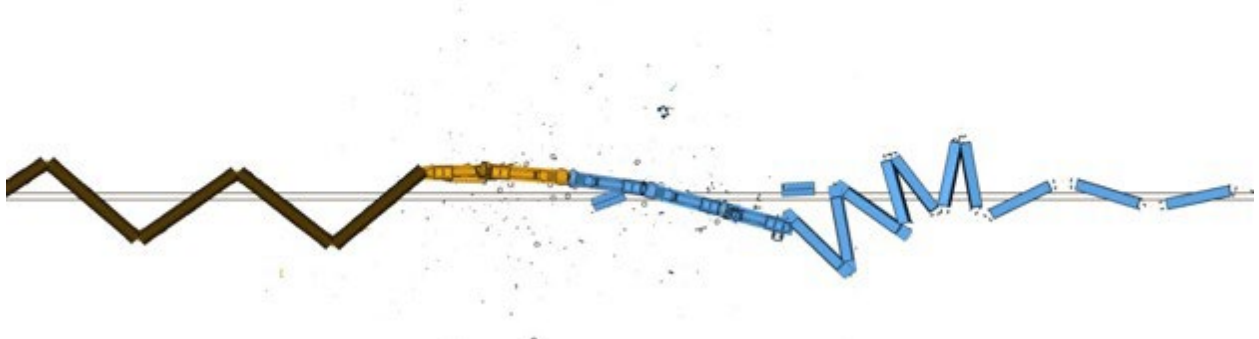


Figure 70. FE Simulation Results, 8 seconds

1: LS-DYNA user input
Loadcase 1 : Time = 9.000011 : Frame 45



Figure 71. FE Simulation Results, 9 seconds

1: LS-DYNA user input
Loadcase 1 : Time = 10.000034 : Frame 50



Figure 72. FE Simulation Results, 10 seconds

1: LS-DYNA user input
Loadcase 1 : Time = 11.000057 : Frame 55



Figure 73. FE Simulation Results, 11 seconds

1: LS-DYNA user input
Loadcase 1 : Time = 12.000080 : Frame 60

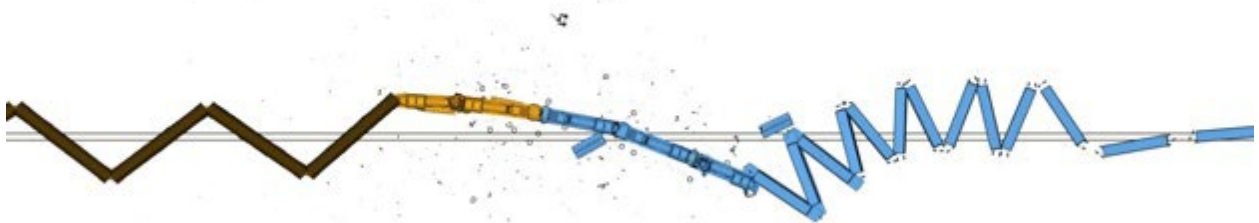


Figure 74. FE Simulation Results, 12 seconds

1: LS-DYNA user input
Loadcase 1 : Time = 13.000103 : Frame 65

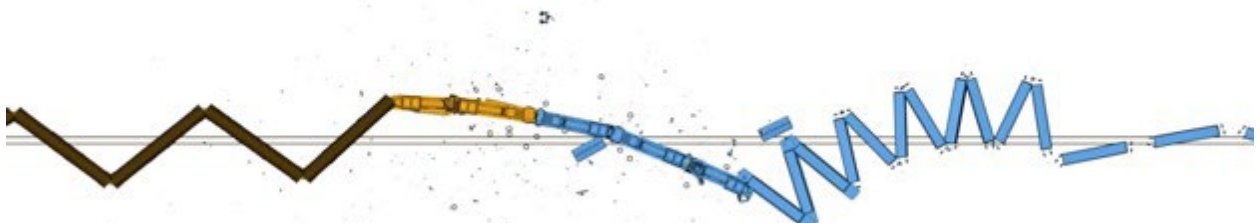


Figure 75. FE Simulation Results, 13 seconds

1: LS-DYNA user input
Loadcase 1 : Time = 14.000126 : Frame 70

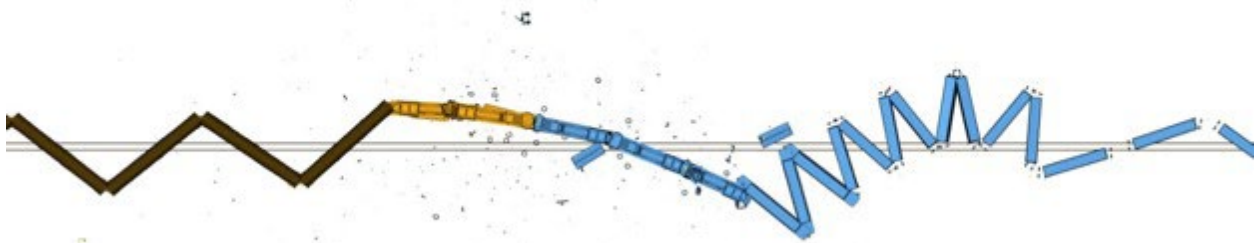


Figure 76. FE Simulation Results, 14 seconds

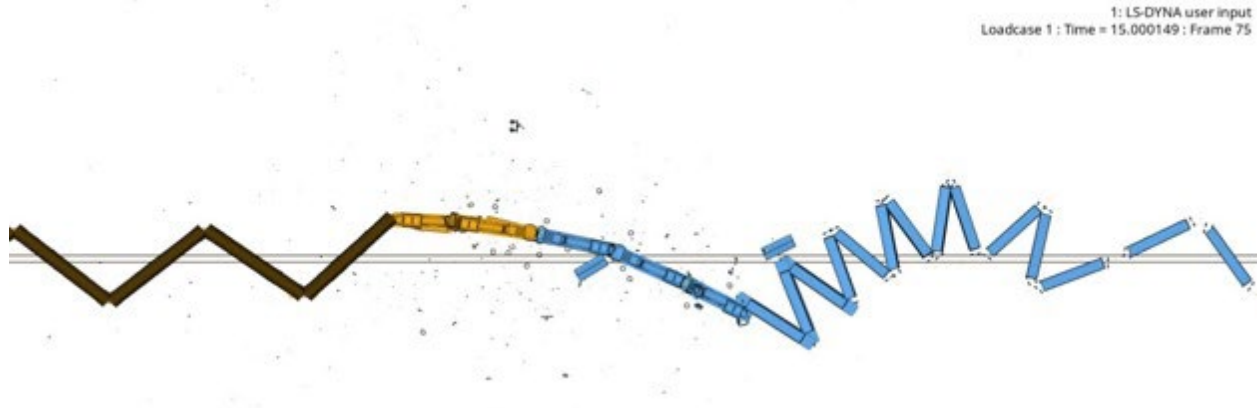


Figure 77. FE Simulation Results, 15 seconds

As previously noted, the NTSB reports lack extensive visual documentation, as their focus is primarily on crash causation. However, the team was able to obtain a few additional post-crash images of the scene to compare side-by-side with the simulation. It should be noted that the simulation stopped at 20 seconds, while the actual crash scene continued beyond that time frame. [Figure 78](#) through [Figure 85](#) present a comparison between crash scenes and the simulation. The locomotives and adjacent road rail cars' behaviors observed in the simulation appear to closely resemble those in the actual test.



Figure 78. NTSB RAR 13-02 Post-Impact Comparison Between the Crash and Simulation, Close-Up of Crash

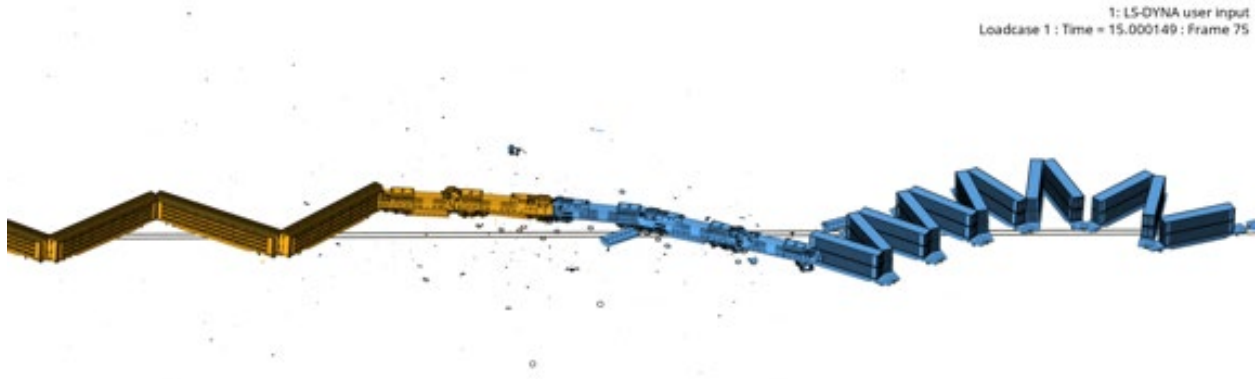


Figure 79. NTSB RAR 13-02 Post-impact Comparison Between the Crash and Simulation, Close-Up Simulation



Figure 80. NTSB RAR 13-02 Post-impact Comparison Between the Crash and Simulation, Close-Up of Crash



Figure 81. NTSB RAR 13-02 Post-impact Comparison Between the Crash and Simulation, Close-Up Simulation



Figure 82. NTSB RAR 13-02 Post-impact Comparison Between the Crash and Simulation, Close-Up of Crash



Figure 83. NTSB RAR 13-02 Post-impact Comparison Between the Crash and Simulation, Close-Up Simulation



Figure 84. NTSB RAR 13-02 Post-Impact Comparison Between the Crash and Simulation, Close-Up of Crash (newschannel10.com)

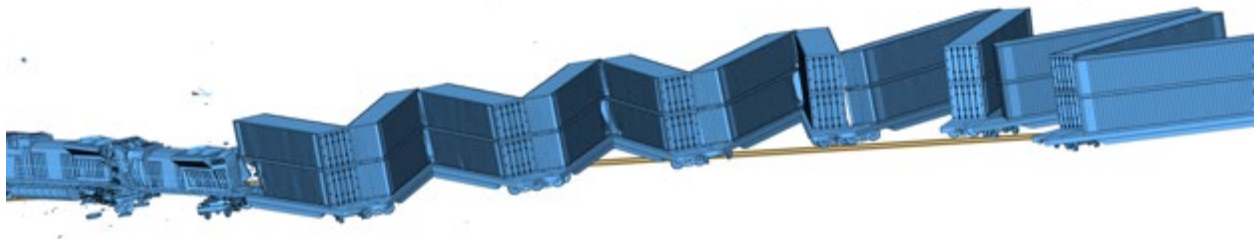


Figure 85. NTSB RAR 13-02 Post-Impact Comparison Between the Crash (Source from newschannel10.com) and Simulation, Close-up

Energies

Figure 86 displays the energy balance of the simulation. The total energy remained stable for the initial 5 seconds of the simulation, with a variation of less than 7.2 percent. The hourglass energy remained below 1 percent but went slightly into the negative zone, indicating that the internal energy offset the kinetic energy. This figure suggests that the model operated as anticipated during the simulation, with no unusual effects observed. However, the total energy started to change over time, since the locomotives and freight cars began to derail, resulting in a shift in the overall energy balance.

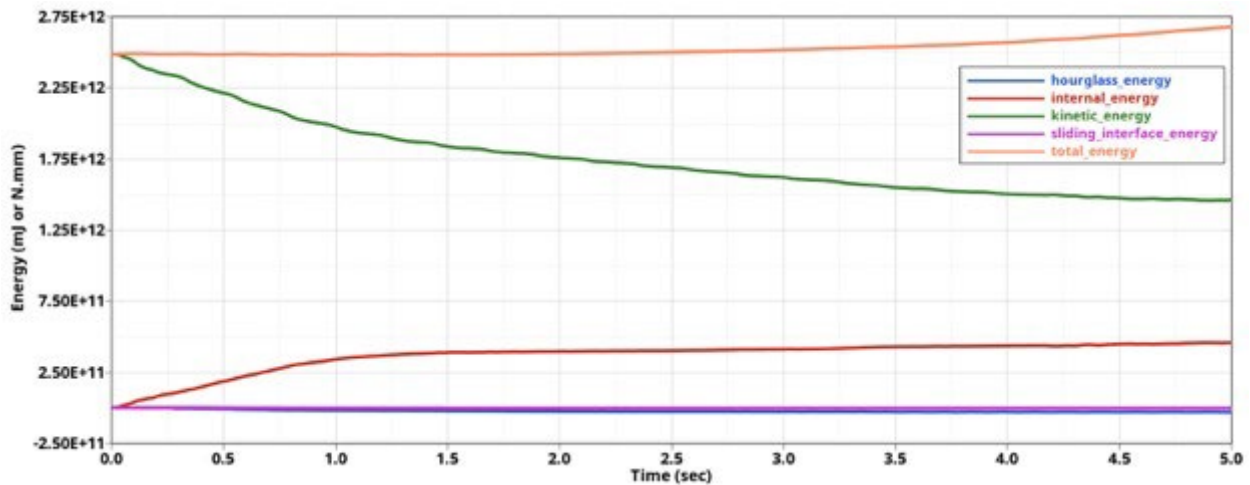


Figure 86. Simulation Energies

5.4 Task 5 Conclusions

In conclusion, the research team conducted a comprehensive review of the NTSB's most significant crash case and made updates to the current FE models, while also designing new models for the train cars that were missing. The simulation was run for a duration of 20 seconds, and the train derailments observed during the simulation demonstrated a satisfactory resemblance to the actual crash site.

6. Task 6

6.1 Research Methodology

The research team proceeded with additional improvements to the FE model and further evaluated the latest S-580 regulations. The subsequent sections provide a detailed description of the steps undertaken during these processes.

6.1.1 Additional Validation of the FE Model

Since the focus of Task 6 was locomotive crashworthiness, the front structure was a crucial area for investigation. During the validation process in Task 4, Test 1 did not exhibit any deformation in the cab section, as it was not reported in the test report. Instead, the locomotive hopped over the open hopper car, resulting in extensive damage to the car, while the locomotive front, frontal truck, and underframe experienced a noticeable damage.

To ensure the inclusion of some cab damage without extensive intrusions into the cab compartment area, the research team re-evaluated all the TTC tests. Two tests were identified as having direct damage to the frontal structure. Test 3 involved a head-on impact with a 35,000-lb steel coil-loaded trailer at a speed of 58 mph, while Test 6 involved an elevated, offset 40-ft intermodal container weighing 65,900 lb, impacting the locomotive at 60 mph. Test 3 resulted in significant damage to the frontal cab structure, whereas Test 6 exhibited localized moderate damage to the frontal cab structure and the windshield post of the cabin area. Since this task aimed to address locomotive crashworthiness, the moderate damage observed in Test 6 was considered more relevant than the excessive damage observed in other tests.

Model SetUp Summary

Test 6 involved a locomotive and three consist cars colliding with a stationary consist at a speed of 60 mph. The stationary consist was comprised of an elevated, offset 40-ft intermodal container weighing 65,900 lb (29.9 tons). [Figure 87](#) shows the original test setup.

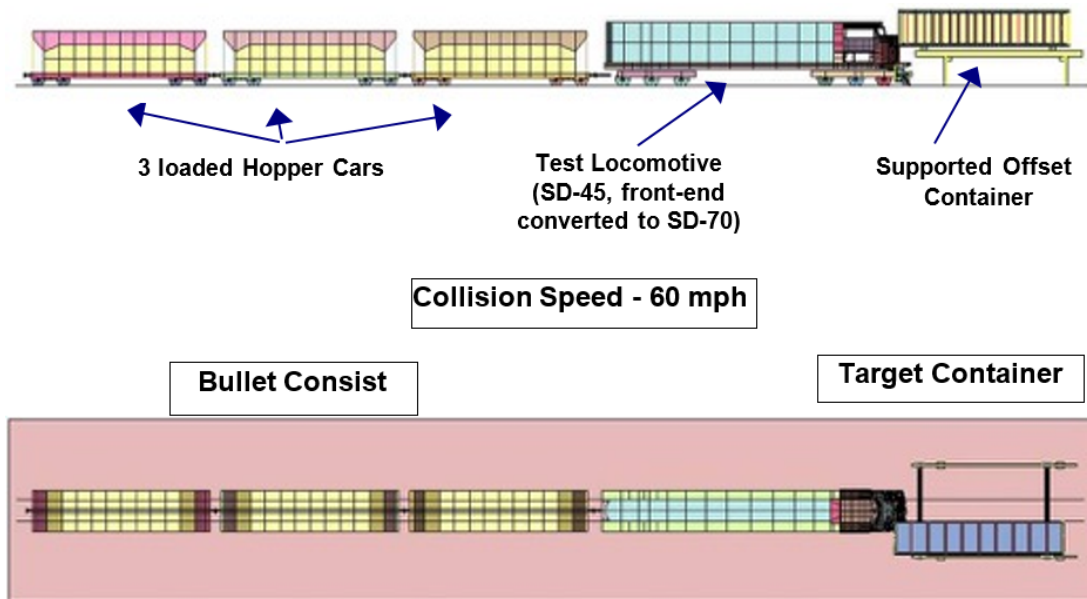


Figure 87. Original Model Set-up (From Test 6 Report)

The FE model was configured to replicate the test setup, following the same methodology as the previous tasks. The locomotive and the three bullet consist cars were modeled in a similar fashion, with respective weights of 379,450 lb (172.2 tons), 262,700 lb (119.2 tons), 257,700 lb (116.9 tons), and 257,750 lb (119.2 tons). The intermodal container weighed approximately 65,900 lbf (29.9 tons). A side-by-side view of the models is depicted in [Figure 88](#) through [Figure 90](#).



Figure 88. Test 6 Pre-Impact Comparison

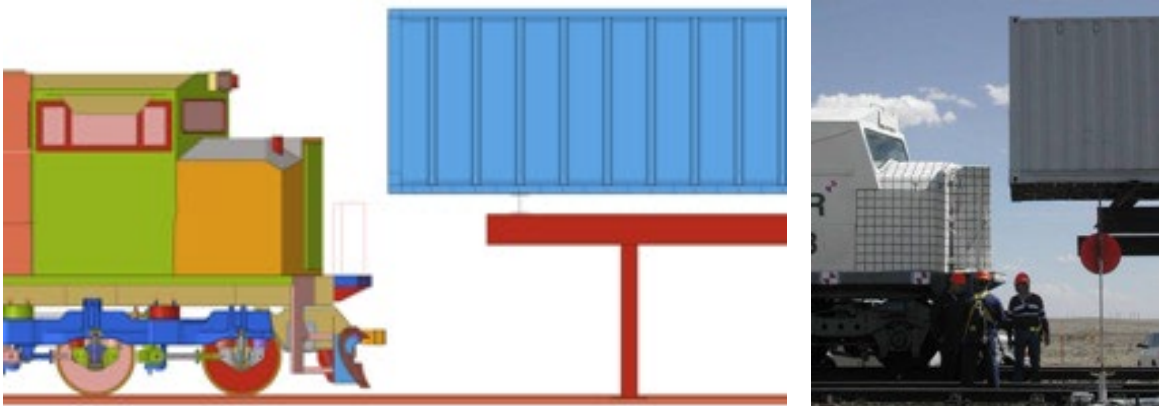


Figure 89. Test 6 Pre-Impact Comparison

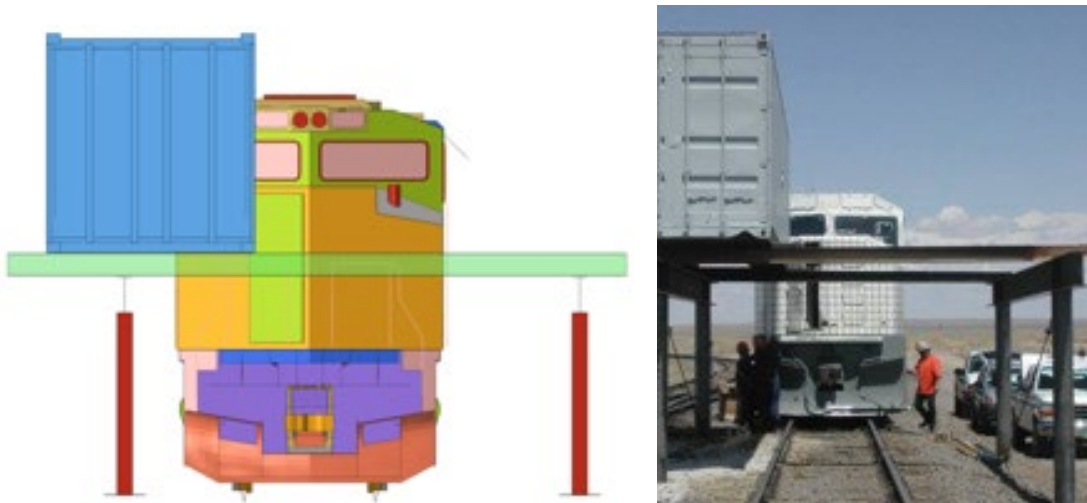


Figure 90. Test 6 Pre-Impact Comparison

Simulation Comparison

The FE model was simulated based on the setup described in the previous section and the TTC test. The subsequent sections discuss the key findings and results.

Key Validation Comparisons

The sequential side-by-side views presented in [Figure 91](#) through [Figure 93](#) showcase the top view test images of the impact zone, obtained from the report. There is a remarkable similarity in behavior between the locomotive and the elevated intermodal container in the simulation and crash test impact.

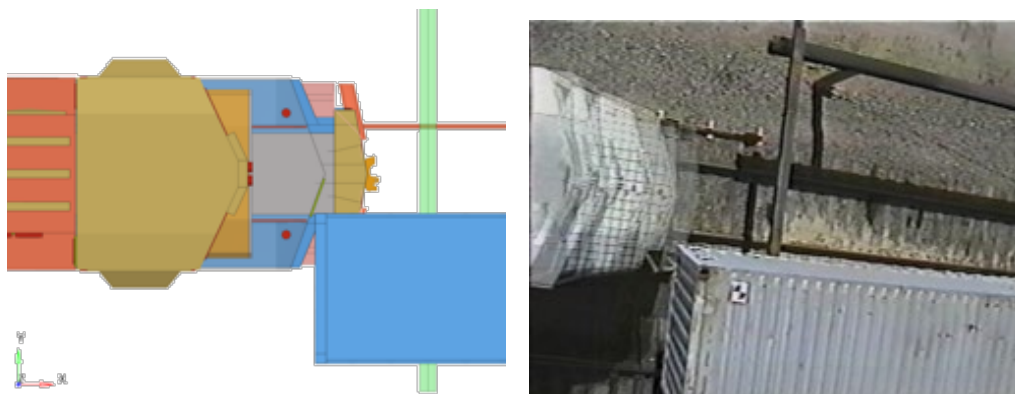


Figure 91. Sequential Images between Simulation and TTC Crash Test, Top View at 100 ms

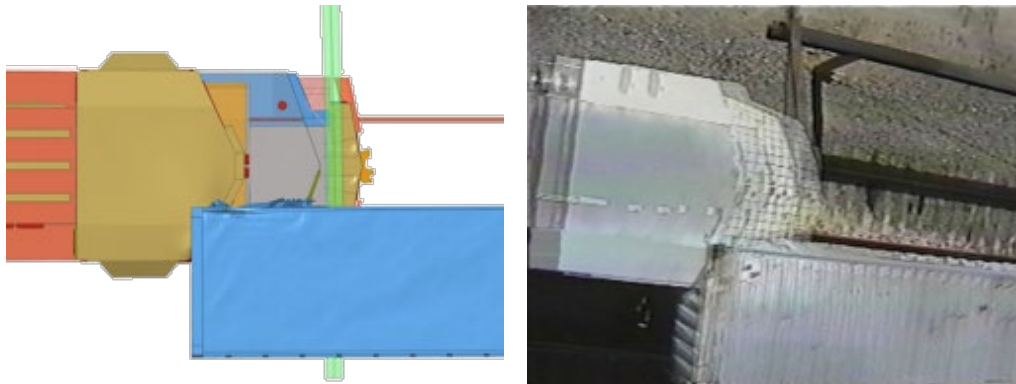


Figure 92. Sequential Images between Simulation and TTC Crash Test, Top View at 200 ms

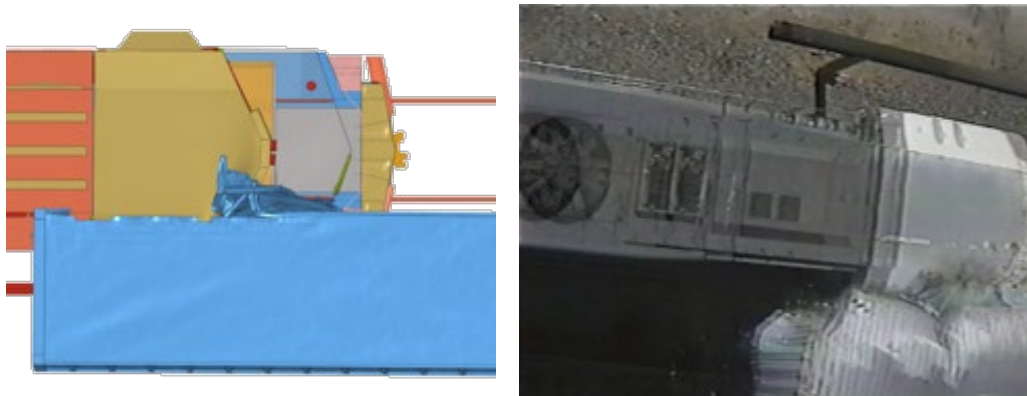


Figure 93. Sequential Images between Simulation and TTC Crash Test, Top View at 300 ms

The team conducted a review of additional online materials related to train tests and discovered valuable videos on YouTube.com. They came across a video titled [128. Train Crash Tests Compilation](#) by “00crashtest”. The video included footage of several TTC tests captured by high-speed video cameras; most can be observed from 5 minutes and 14 seconds until the end of the clip, which is 11 minutes and 34 seconds long.

Despite the low video quality, the unknown frame rate of the slow-motion footage, and poor test descriptions, the research team managed to visually compare the tests and gather additional side-by-side comparisons. However, due to the similarity between Tests 6 and 9, it was challenging to differentiate which one was shown in the video. Nevertheless, [Figure 94](#) through [Figure 101](#) illustrate different comparison views based on the available footage.

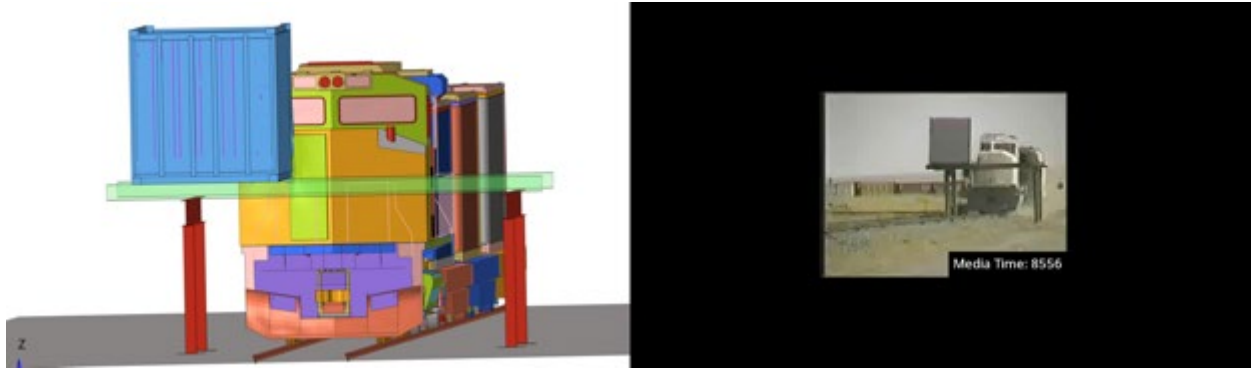


Figure 94. Sequential Images between Simulation and TTC Crash Test, Front View at 100 ms

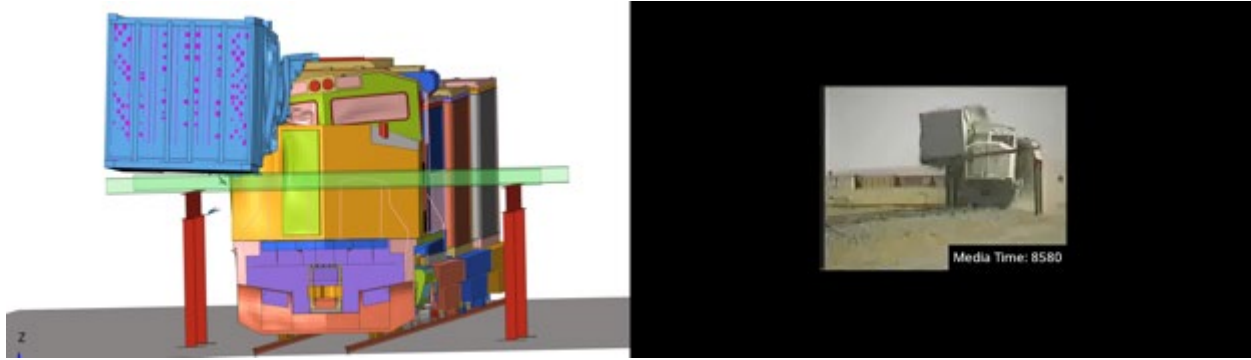


Figure 95. Sequential Images between Simulation and TTC Crash Test, Front View at 200 ms

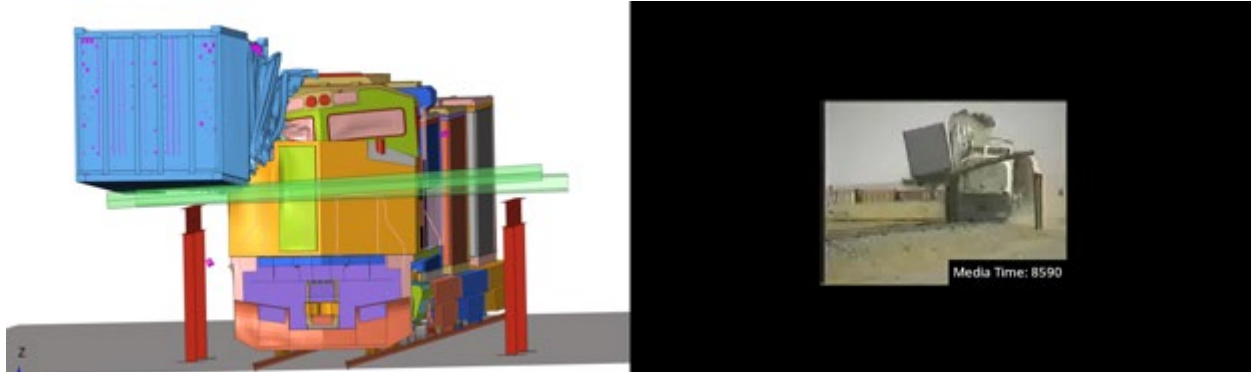


Figure 96. Sequential Images between Simulation and TTC Crash Test, Front View at 300 ms

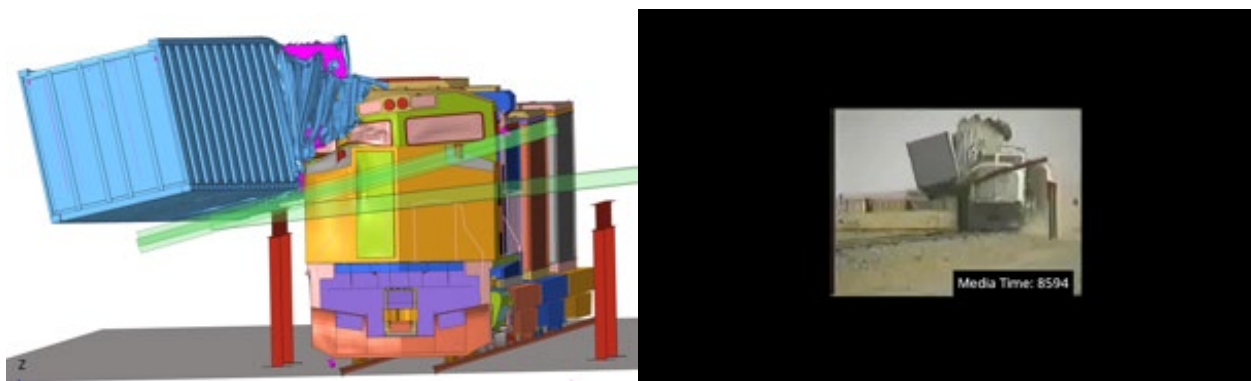


Figure 97. Sequential Images between Simulation and TTC Crash Test, Front View at 400 ms

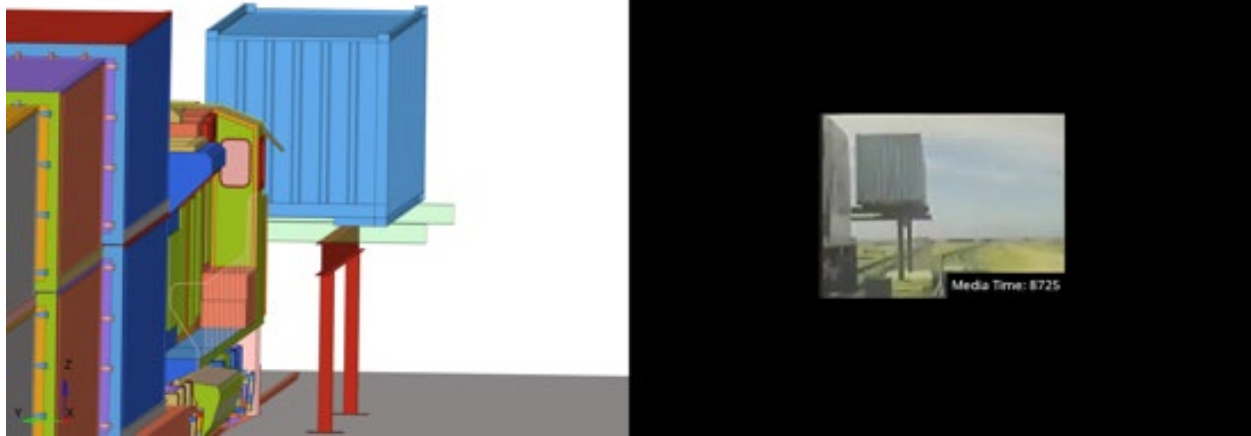


Figure 98. Sequential Images between Simulation and TTC Crash Test, Rear View at 100 ms



Figure 99. Sequential Images between Simulation and TTC Crash Test, Rear View at 200 ms

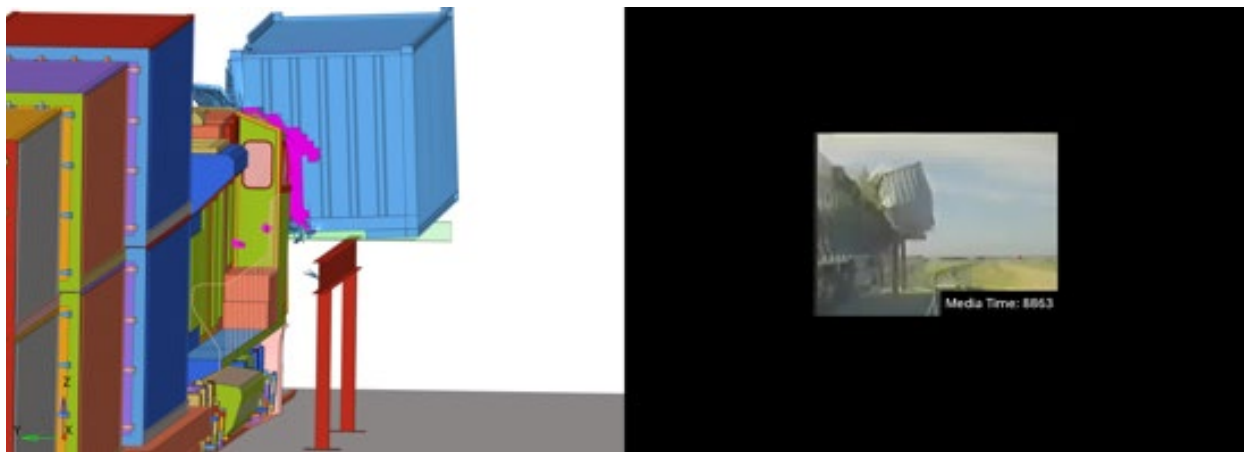


Figure 100. Sequential Images between Simulation and TTC Crash Test, Rear View at 300 ms

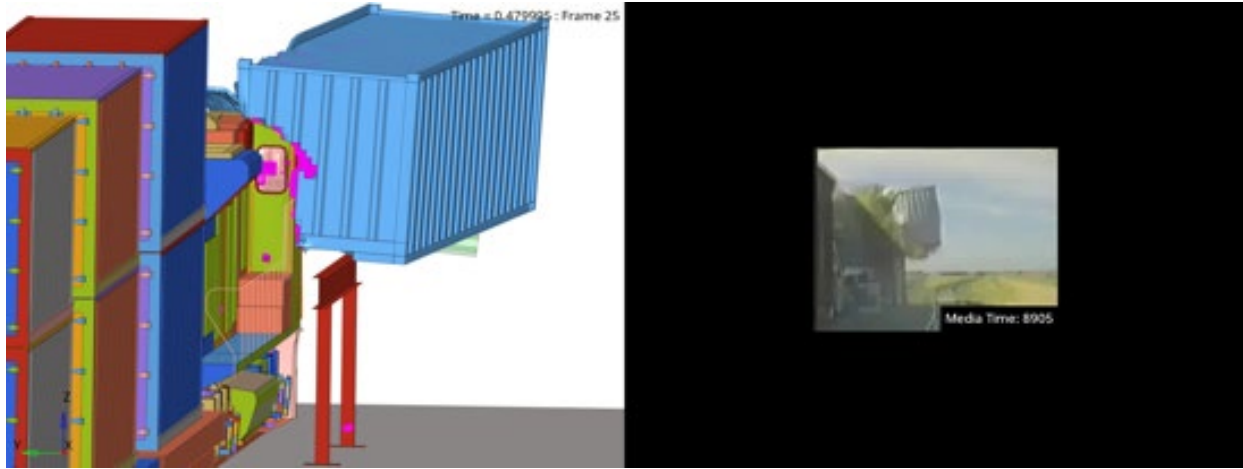


Figure 101. Sequential Images between Simulation and TTC Crash Test, Rear View at 400 ms

Photographs comparing the test and simulation post-impact are displayed in [Figure 102](#) through [Figure 104](#). The test pictures depict the extent of damage sustained by the locomotive and the container. The simulation successfully captured a similar tearing behavior. While the container in the test fell to the ground, the simulation exhibited comparable crush behavior, although it did not reach the ground. Note that the simulation only covered a single second of the crash test, and there was still forward motion of the locomotive and falling motion of the container beyond that timeframe. Considering that this task specifically focused on the locomotive loading, longer simulation times were deemed irrelevant and not included.



Figure 102. Post-Impact Crush Comparison

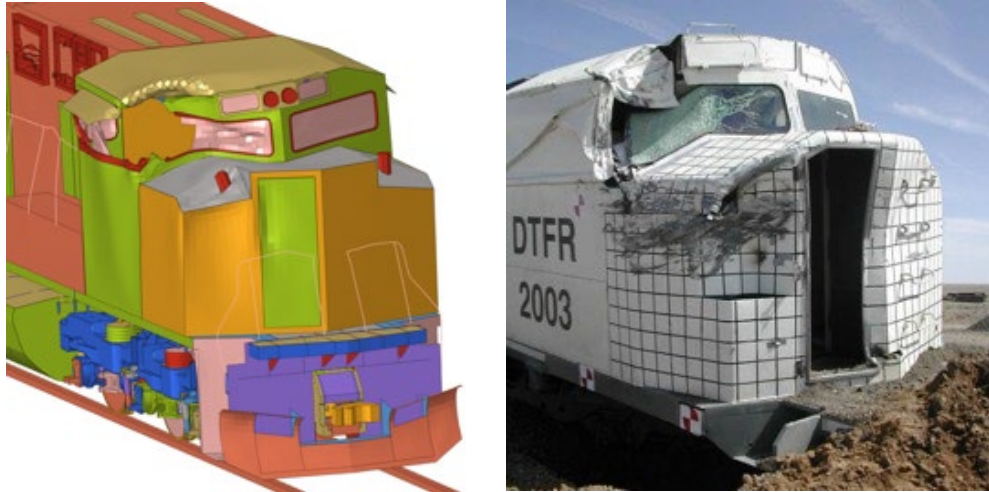


Figure 103. Post-Impact Crush Comparison

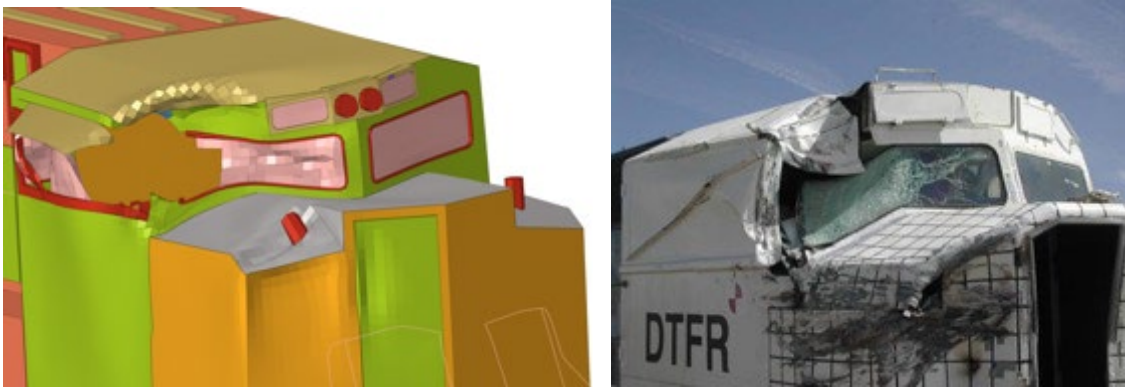


Figure 104. Post-Impact Crush Comparison

Energies

Figure 105 shows the energy balance of the simulation. The total energy remained stable, with a variation of less than 0.2 percent. The hourglass energy accounted for 1.7 percent of the total energy throughout the 1-second simulation. This energy distribution signifies a balance between internal energy and contact/sliding energy, effectively offsetting the kinetic energy.

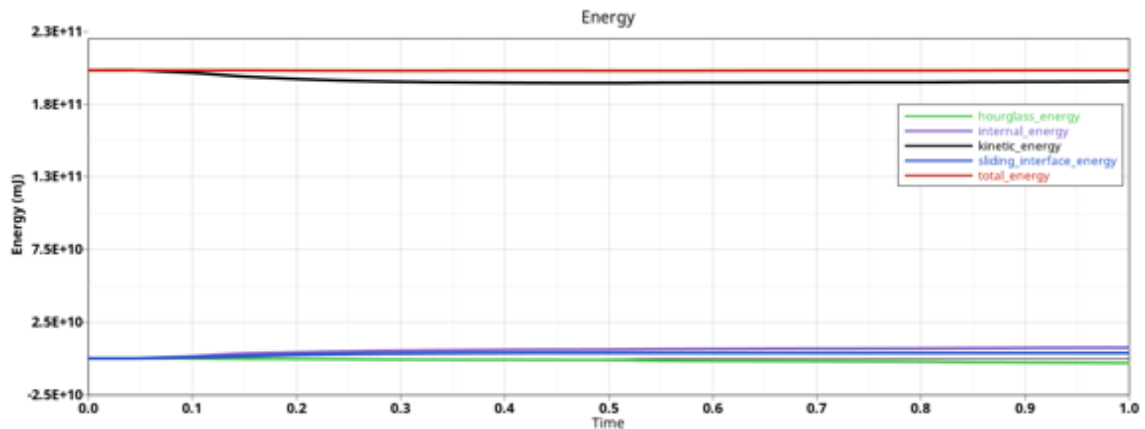


Figure 105. Simulation Energies

The figure indicates that there were no anomalous effects, suggesting that the model performed as expected during the simulation. The consistent energy balance observed reinforces the reliability of the simulation results.

6.1.2 S-580 Regulations Performance Criteria

The FRA S-580 regulations outline specific locomotive crashworthiness requirements and performance criteria to improve crew-safety in the event of collisions or accidents, including structural design, energy absorption, crew-safety protection, and intrusion limits. The following sections focus on two key elements of the S-580 regulations: the dynamic aspect and the quasi-static loads of the collision posts, which both relate directly to the locomotive cab intrusion.

Collision Post Static Loading

The collision posts play a critical role in absorbing crash energy during in-line train-to-train collisions or impacts with large motor vehicles. In accordance with the S-580 minimum standards, the collision posts are required to withstand specific force applications. These requirements include withstanding 750,000 lb of force at the point of attachment and 500,000 lb of force applied at a point 30 in above the top of the underframe. In previous S-580 regulations, the requirements were set at 500,000 lb at 30 in above the underframe and 200,000 lb at the base of the collision post.

To assess the performance of the collision posts, the team applied static loads to the right-side post of the FE model while the locomotive was not allowed to move. [Figure 106](#) illustrates the Von Mises stresses on the collision post, with the hood made transparent to reveal the loading details. Although the lower loading appears to approach the plastic phase, no element failures was observed. The localized red element is considered acceptable given the large size of the elements used in the analysis (2.6 in/67 mm).

Overall, the FE model analysis indicates that the collision posts are able to withstand the required static loads and demonstrate satisfactory stress distribution, ensuring their effectiveness in absorbing crash energy during collisions or impacts.

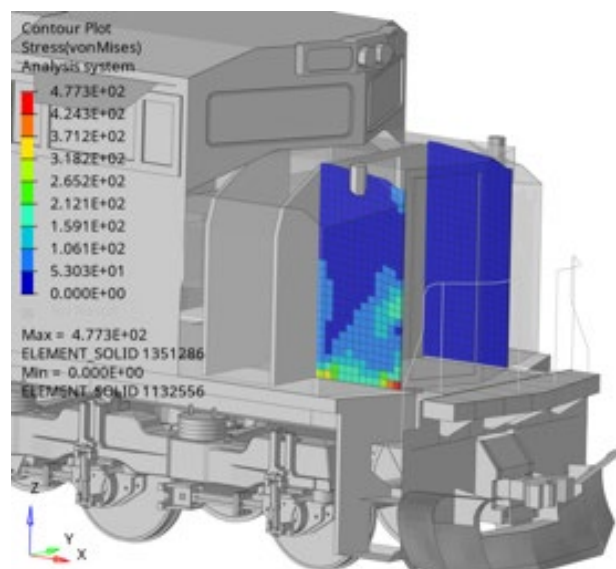


Figure 106. S-580: 750,000/500,000 Collision Post Loading

Dynamic Performance

The dynamic performance criteria for evaluating the crashworthiness of locomotive designs outlined in S-580 consist of two tests. Each criterion defines a collision scenario and specifies a performance measure to evaluate the protection provided to cab crews through structural design. The details of both criteria are addressed in the following sections.

Cylindrical Object at 30 mph (Head-On)

To assess the front-end structure of the locomotive, a crash test was conducted using a cylindrical proxy object (Appendix E-a in S-580). The cylindrical shape had a diameter of 48 in, a length of 126 in, and a minimum weight of 65,000 lb (29.5 tons). The objective of the test was to verify that the front-end structure could withstand a 30-mph impact with the cylindrical shape, resulting in a maximum crush of no more than 24 in along the longitudinal axis of the locomotive. The test setup, as specified by the regulation, is depicted in [Figure 107](#).

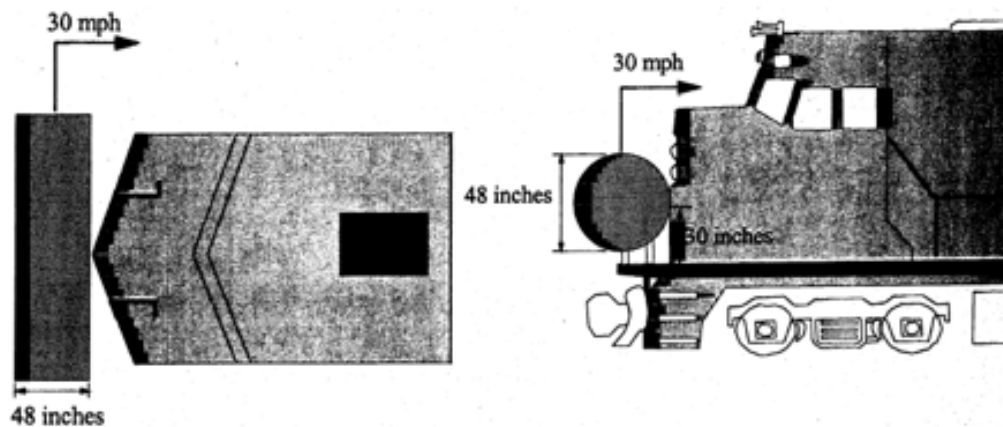


Figure 107. S-580: Cylindrical Shape of 126 in (length) at 30 mph

Following the test, the FE model was simulated based on the described setup. [Figure 108](#) through [Figure 111](#) present sequential side views of the impact zone. The maximum intrusion caused by the cylindrical shape was 16.38 in. This value falls below the specified requirements, indicating that the front-end structure of the locomotive meets the standards outlined by the regulations. Overall, the evaluation of the front-end structure using the cylindrical proxy object demonstrates that the locomotive design successfully meets the dynamic performance criteria set forth in S-580, ensuring the appropriate protection of cab crews during collisions.



Figure 108. S-580: Cylindrical Shape Simulation Sequential Images at 0 ms



Figure 109. S-580: Cylindrical Shape Simulation Sequential Images at 150 ms



Figure 110. S-580: Cylindrical Shape Simulation Sequential Images at 200 ms

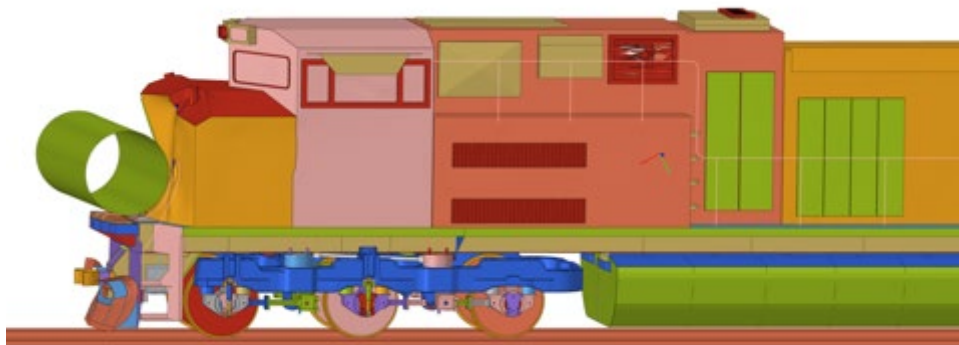


Figure 111. S-580: Cylindrical Shape Simulation Sequential Images at 250 ms

Rectangular Object at 30 mph with 12 in Overlap

The second specified testing scenario for the front-end structure of the locomotive used a rectangular proxy object (S-580 Appendix E-b). The rectangular shape had a width of 36 in, height of 60 in, length of 108 in, and a minimum weight of 65,000 lb (29.5 tons). The objective of the test was to ensure that the front-end structure of the locomotive could withstand a 30 mph impact from the rectangular shape, resulting in a maximum crush of no more than 60 inches along the longitudinal axis of the locomotive. The test setup, as outlined in the regulation, is depicted in [Figure 112](#).

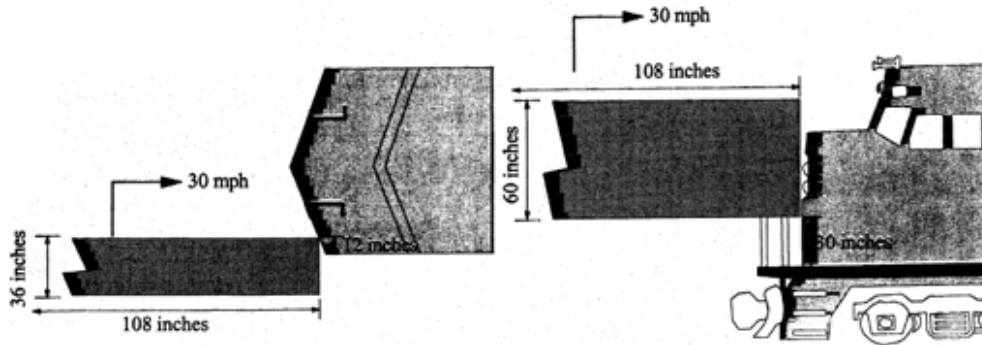


Figure 112. S-580: Rectangular Shape Offset by 12 in at 30 mph

Following the test, the FE model was simulated based on the specified setup. [Figure 113](#) through [Figure 116](#) illustrates sequential side views of the impact zone. The analysis determined that the maximum intrusion caused by the rectangular shape was measured at 14.2 inches. This value falls below the specified requirements, indicating that the front-end structure of the locomotive successfully meets the standards established by the regulations.

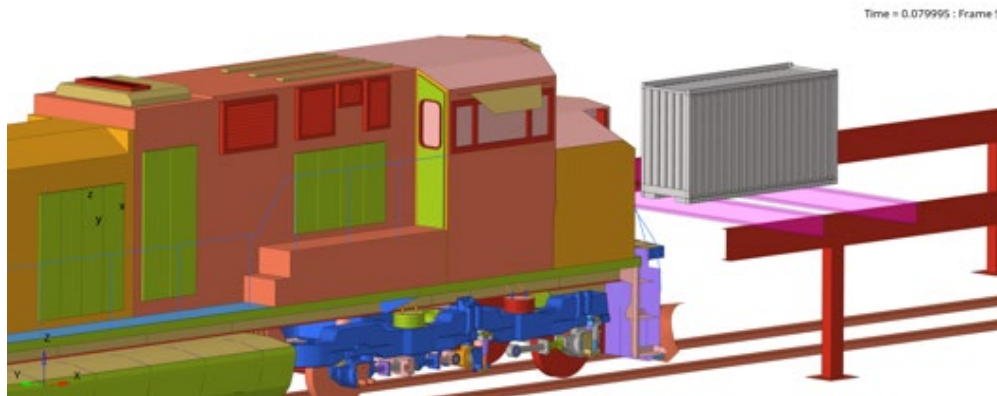


Figure 113. S-580: Rectangular Shape Simulation Sequential Images at 0 ms

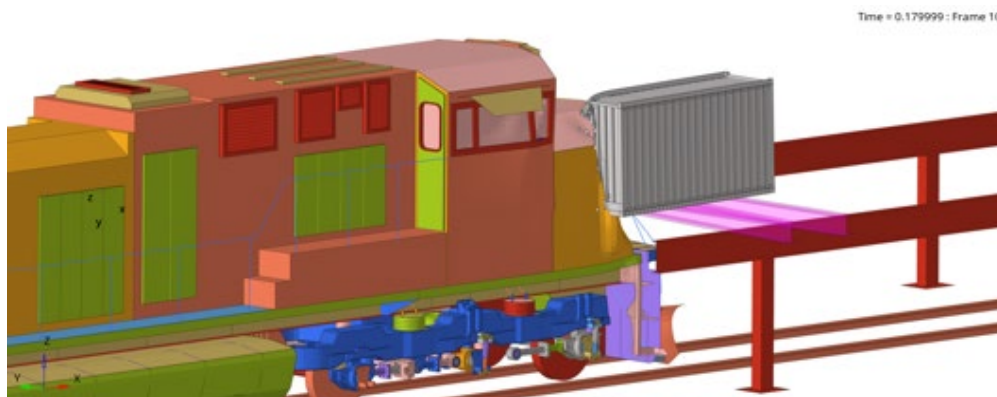


Figure 114. S-580: Rectangular Shape Simulation Sequential Images at 100 ms



Figure 115. S-580: Rectangular Shape Simulation Sequential Images at 220 ms



Figure 116. S-580: Rectangular Shape Simulation Sequential Images at 420 ms

In summary, the evaluation of the front-end structure using the rectangular proxy object confirms that the locomotive design satisfies the dynamic performance criteria outlined in the S-580 regulations. The structure demonstrates its ability to withstand a 30 mph impact with the rectangular shape, ensuring that the crush deformation remains within the specified limits, thus enhancing the crashworthiness of the locomotive.

Overall Performance

The inclusion of the additional TTC crash Test 6 validation and the dynamic evaluation based on S-580 has led to notable enhancements in the FE model of the locomotive, with a specific focus on the locomotive cab structure. These updated findings and refinements were added to the locomotive FE model.

6.2 Evaluation of S-580 Regulation Impact for Previous years

After reviewing NTSB cases, the research team determined that these cases could not be used for the new S-580 regulations crashworthiness assessment. Some cases occurred at high speeds, while others lacked necessary data to assess crew-safety cab safety adequately.

To quantitatively compare the impact of the S-580 regulations on modern locomotive crashworthiness compared to non-modern locomotives, the research team proposed conducting dynamic loading test using a cylindrical object (as described in [Section 6.1.2.2](#)) on older locomotives. The goal is to compare the dynamic intrusions between modern and non-modern

locomotives. The strength of the collision posts plays a crucial role in determining the level of intrusion into the locomotive cab.

Since the team was unable to obtain specifications or models for non-modern locomotives, they considered using the latest FE model developed to calculate their collision post thickness. This was achieved by applying the previous year's regulation static loading to estimate the collision post thicknesses.

The following sections provide a comprehensive description of the proposed assessments, focusing on the dynamic and static evaluations and their implications for modern locomotive crashworthiness.

6.2.1 S-580 Regulations Performance Criteria for Previous years

In accordance with previous S-580 minimum standards, the collision posts are required to withstand specific force applications. These requirements include withstanding 500,000 lb of force at the point of attachment and 200,000 lb of force applied at a point 30 inches above the top of the underframe.

Collision Post Static Loading for Previous Regulations

To determine the collision post thickness, static loads based on previous locomotive regulations were applied to the right-side post of the FE model while the locomotive was immobilized. This approach was chosen due to the lack of available data on older locomotives. The team achieved this by adjusting the collision post thickness iteratively until it met the required loads (500,000/200,000 lb).

Through iterative analyses, the collision post thickness based on previous locomotives regulations was calculated to be about 1/3 of the original model's thickness. [Figure 117](#) illustrates the Von Mises stresses on the collision post, with the hood made transparent to reveal the loading details. The lower loading on the weaker collision post appears to meet the older S-580 requirements.

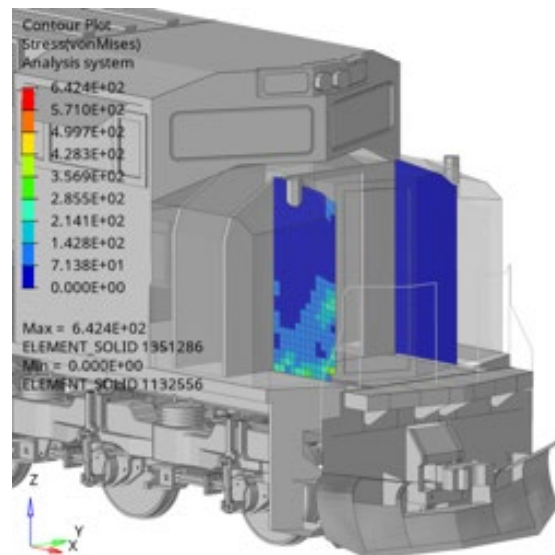


Figure 117. S-580: 500,000/200,000 Collision Post Loading for Previous Locomotive Regulations

Cylindrical Object at 30 mph (Head-On) for Previous Regulations

Similarly, the FE model of non-modern locomotive was simulated based on the setup described in Section 6.1.2.2. Figure 118 through Figure 121 provide sequential side views of the impact zone. The maximum intrusion caused by the cylindrical shape was 27.58 in, exceeding the specified requirement of 24 in. This indicates that the front-end structure of the non-modern locomotive had a front cab penetration that was over 68 percent greater than the modern locomotive cab intrusion for a cylindrical proxy object.



Figure 118. S-580: Cylindrical Shape Simulation Sequential Images for non-modern Locomotive Regulations at 0 ms



Figure 119. S-580: Cylindrical Shape Simulation Sequential Images for non-modern Locomotive Regulations at 150 ms



Figure 120. S-580: Cylindrical Shape Simulation Sequential Images for non-modern Locomotive Regulations at 200 ms

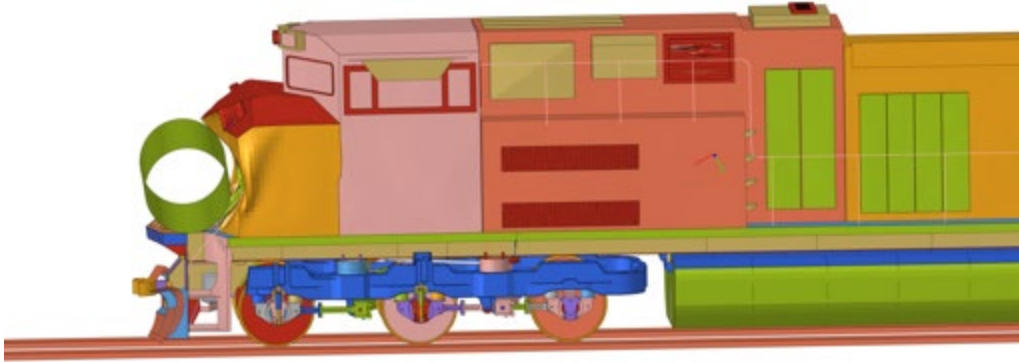


Figure 121. S-580: Cylindrical Shape Simulation Sequential Images for non-modern Locomotive Regulations at 250 ms

6.2.2 S-580 Regulation of 2005 Evaluation

Overall, the evaluations of the front-end structure using the cylindrical proxy object demonstrate that modern locomotive designs based on the new S-580 regulations offer better crew safety compared to previous regulations and older (non-modern) locomotives. The new S-580 regulations ensure better protection for cab crews during collisions compared to previous S-580 regulations.

7. Conclusions

The Final Rule that FRA established in 2009 ushered in a new standard for locomotive compliance. To be deemed "modern," locomotives must meet both the new federal standard and the crashworthiness requirements outlined in the AAR S-580-2005 guidelines. Locomotives manufactured before 2009 are classified as "not modern" for the purposes of this study.

This project aims to assess the impact of the AAR S-580 requirements on modern locomotive crashworthiness, utilizing a combination of statistical analysis and FE modeling and simulations. The statistical analysis delves into real-world crash data, while the modeling endeavors to enhance train car and locomotive models, validate them against existing crash tests, and evaluate their crashworthiness in accordance with the S-580 requirements through simulations.

In the initial phase, the research team examined the FRA Accident and Incident Database and the NTSB Accident and Incident Database for freight train collisions and derailments involving modern locomotives with in-cab occupant casualties. The team then developed collision evaluation criteria by employing a ranking metric and weighting factor to identify the most severe collision cases. Severity was determined based on operational parameters such as collision type and closing speed, with crew casualties serving as indicators of severity.

In the modeling phase, the research team upgraded all FE models by enhancing mesh, connections, materials, and properties, drawing on the team collective experience in automotive safety and utilizing publicly available information. The research team validated the models through train crash simulations, using TTC crash tests for validation purposes. These models were subsequently used to simulate the NTSB cases identified as the most severe.

Another aspect of the modeling phase involved simulating the static and dynamic requirements of the AAR S-580 guidelines, focusing on comparing the crashworthiness of modern and non-modern locomotives. The analysis revealed that modern locomotives exhibit significantly less front cab penetration compared to non-modern locomotives when subjected to the requirements of the AAR S-580 guidelines, specifically for cylindrical proxy objects.

In conclusion, this study underscores that the latest FRA train crashworthiness standards offer increased safety for crew compartments compared to older regulations. The modern designs provide better protection for the crew during crashes, enhancing their overall safety and minimizing the risk of injuries.

References

- Association of American Railroads. (2020). *MSRP Section M - Locomotives and Locomotive Interchange Equipment*.
- Craig, R. [Locomotive Rosters](#). The Diesel Shop. Retrieved September 1, 2021.
- [Locomotive Crashworthiness](#), 71 FR 36888 (2006).
- National Technical Information Service. [National Technical Reports Library](#). Retrieved September 1, 2021.
- U.S. Department of Transportation. [Class I Railroad Locomotive Fleet by Year Built](#). Bureau of Transportation Statistics. Retrieved December 14, 2020.
- U.S. Federal Railroad Administration. [Accident/Incident Dashboards & Data Downloads](#). FRA Safety Data and Reporting. Retrieved September 1, 2021.
- U.S. National Transportation Safety Board. [Investigation Reports](#). Retrieved September 1, 2021.
- Xin, X., Parida, B., Zaouk, A., Dana, N., & Punwani., S. (2012, June). [Impact Analysis of an Innovative Shock Energy Absorber and Its Applications in Improving Railroad Safety](#). 12th International LS-DYNA Users Conference, Detroit, MI.

Abbreviations and Acronyms

ACRONYMS	EXPLANATION
AAR	Association of American Railroads
CFR	Code of Federal Regulations
FE	Finite Element
FEA	Finite Element Analysis
FRA	Federal Railroad Administration
MOW	Maintenance of Way
NTIS	National Technical Information Service
NTSB	National Transportation Safety Board
RSAC	Railroad Safety Advisory Committee
TTC	Transportation Technology Center